TECHNICAL REPORT STANDARD TITLE PAGE

1. Report No.	2. Government Accession No.	3. Recipient's Catalog No.
CFHR 3-8-71-156-2		

4. Title and Subtitle	5. Report Date
"The Use of Spectral Estimates for Pavement Characterization"	August 1973
	6. Performing Organization Code
7. Author(s)	8. Performing Organization Report No.
Roger S. Walker and W. Ronald Hudson	Research Report 156-2
9. Performing Organization Name and Address	10. Work Unit No.
Center for Highway Research The University of Texas at Austin Austin, Texas 78712	11. Contract or Grant No. Research Study 3-8-71-156
	13. Type of Report and Period Covered
12. Sponsoring Agency Name and Address	Interim Feb. 1973 - Aug. 1973
Texas Highway Department 11th and Brazos Austin, Texas 78701	14. Sponsoring Agency Code

15. Supplementary Notes

Research performed in cooperation with Department of Transportation, Federal Highway Administration.
Research Study Title: "Surface Dynamics Road Profilometer Applications"

16. Abstract

An investigation of the uses of road profile spectral estimates for characterizing pavements has been made and is reported herein. This investigation included the development of a serviceability index prediction model based entirely on the road profile wavelength amplitude estimates. This model has been used extensively in both research and field operations and is also currently being used as the SI model standard for Mays Road Meter calibration procedures. Other pavement characterization techniques are also discussed, including the use of digital filtering techniques for obtaining more comprehensive wavelength-amplitude descriptors.

17. Key Words	18. Distribution Statement
Surface Dynamics Road Profilometer, serviceability index, road profile amplitude spectrum, digital filtering.	

19. Security Classif. (of this report)	20. Security Classif. (of this page)	21. No. of Pages	22. Price
Unclassified	Unclassified	72	

Form DOT F 1700.7 (8-69)

THE USE OF SPECTRAL ESTIMATES FOR PAVEMENT CHARACTERIZATION

by

Roger S. Walker
W. Ronald Hudson

Research Report Number 156-2

Surface Dynamics Road Profilometer Applications
Research Project 3-8-71-156

conducted for

The Texas Highway Department

in cooperation with the
U. S. Department of Transportation
Federal Highway Administration

by the

CENTER FOR HIGHWAY RESEARCH
THE UNIVERSITY OF TEXAS AT AUSTIN

August 1973

The contents of this report reflect the views of the authors, who are responsible for the facts and the accuracy of the data presented herein. The contents do not necessarily reflect the official views or policies of the Federal Highway Administration. This report does not constitute a standard, specification, or regulation.

PREFACE

This is the second report presenting results from Research Project 3-8-71-156, "Surface Dynamics Road Profilometer Applications," which was initiated to carry out the implementation and operation of the Surface Dynamics (SD) Road Profilometer in field and research applications.

The SD Profilometer measuring system was initially developed under Research Project 3-8-63-73, "Development of a System for High-Speed Measurement of Pavement Roughness." A set of serviceability index prediction equations was also developed during that project, from the results of a large-scale rating session of typical Texas pavements. The current project involves the implementation of many of the research results from Project 3-8-63-73. This report discusses the uses of the original rating session data from Project 73 in correlating pavement serviceability ratings with the road profile amplitude estimates and the extensive uses of this model in field and research applications. The development and uses of some other analysis techniques are also discussed.

The assistance of Texas Highway Department Contact Representative James L. Brown is especially appreciated. The authors also wish to acknowledge the assistance of Center for Highway Research personnel H. H. Dalrymple and Hugh Williamson.

Roger S. Walker
W. Ronald Hudson

August 1973

LIST OF REPORTS

Report No. 156-1, "A Correlation Study of the Mays Road Meter with the Surface Dynamics Profilometer," by Roger S. Walker and W. Ronald Hudson, discusses a study of the correlation between measurements made with the Mays Road Meter and the Surface Dynamics Profilometer and, based on this study, provides a set of calibration, operation, and control procedures for operation of the Mays Road Meter using serviceability index values from the profilometer as a measurement standard.

Report No. 156-2, "The Use of Spectral Estimates for Pavement Characterization," by Roger S. Walker and W. Ronald Hudson, discusses the general uses of road profile spectral estimates for pavement characterization. A model for predicting serviceability index based on road profile amplitude estimates is also described.

ABSTRACT

An investigation of the uses of road profile spectral estimates for characterizing pavements has been made and is reported herein. This investigation included the development of a serviceability index prediction model based entirely on the road profile wavelength amplitude estimates. This model has been used extensively in both research and field operations and is also currently being used as the SI model standard for Mays Road Meter calibration procedures. Other pavement characterization techniques are also discussed, including the use of digital filtering techniques for obtaining more comprehensive wavelength-amplitude descriptors.

KEY WORDS: Surface Dynamics Road Profilometer, serviceability index, road profile amplitude spectrum, digital filtering.

SUMMARY

The problem of obtaining comprehensive pavement characterizing statistics which can be effectively related to pavement roughness, performance, and distress has been a prime concern of highway engineers. Slope variance and condition survey measurements such as patching, cracking, and rut depth have made up one of the most widely used set of such statistics, or variables, for pavement performance measurements. This report describes research performed in which road profile wavelength amplitude estimates have been successfully used as pavement characterizing statistics, and in particular for obtaining pavement serviceability and performance measurements. The SD Profilometer provides a practical means by which accurate road profile information can be rapidly obtained, thus making possible the effective utilization of road profile wavelength amplitude statistics. The serviceability index (SI) model which is a function of the amplitude statistics is currently being implemented by the Texas Highway Department both for SI measurements in field and research applications and as the calibration standard for the Mays Road Meter.

Additional discussions include the uses of digital filtering techniques for more comprehensive road profile amplitude investigations. Such methods show promise in providing key pavement descriptor statistics which can possibly be used in relating pavement distress to performance, one of the major concerns of highway design engineers today.

IMPLEMENTATION STATEMENT

A new serviceability index model has been developed which is entirely a function of the road profile amplitude estimates. This model is currently being implemented in obtaining SI measurements for both research and field applications. In addition, it is the model which provides the SI measurement standard for the Mays Road Meter calibration procedures.

TABLE OF CONTENTS

CHAPTER 1. INTRODUCTION

During Project 3-8-63-73, "Development of a System for High-Speed Measurement of Pavement Roughness," serviceability index models were developed (Ref 5), based on the serviceability performance concept of Carey and Irick (Ref 1). The pavement serviceability concept used in Project 73 differed slightly from this initial concept in that it was based entirely on users' subjective evaluations of the riding quality of the pavement at any given time.

For this method, correlations are made between physically representative characteristics of the surface of a set of test pavements and the subjective riding quality of these pavements. The users' subjective evaluations are obtained by averaging the individual present serviceability rating (PSR) values noted by members of a users' rating panel. These rating values are based on a linear scale from zero to five in which a road with a PSR of zero is considered impassable for high-speed traffic and a road with a PSR of five is perfect. This concept has since been used in its original and modified forms to predict pavement serviceability.

Since this concept requires correlation between objective physical measurements of pavement characteristics and subjective evaluations of pavement riding quality by highway users, the development of reliable serviceability index (SI) prediction models is not a trivial task; it requires some type of an adequate statistically designed highway rating experiment for the subjective measurements and some type of roughness measuring device for the objective measurements. The availability of the Surface Dynamics (SD) Profilometer provided a profile measuring device which could be used for obtaining accurate road profile information from which roughness characteristics could be obtained. Then, during Project 73 (Ref 5), a pavement rating experiment was conducted in which a panel of typical road users riding in typical American automobiles expressed their opinions of the riding quality of a group of pavements. Ninety-nine sites for the rating sessions were selected to represent different topographical areas of Texas, and the road profiles of these test pavements,

along with pavement deterioration (conditional survey) information such as the measurements of texture, rut depths, and patching and cracking, were taken with the SD Profilometer. Roughness index and slope variance statistics computed from these data were used for characterizing the pavement sections. These two statistics were selected because of their relationship with features which induce forces on the rider and because of their previous acceptance in the highway field. Roughness index is the sum of the vertical deviations of the profile throughout the section, and slope variance is the variance of slopes calculated for the length of the section.

These roughness statistics and condition survey data were correlated with the mean PSR panel ratings to provide pavement SI prediction models. Later, somewhat better models were obtained through data-centering techniques during the regression analysis (Ref 9).

Several problems were noted in using slope variance as the primary road roughness characterization statistic. For one, it does not individually explain enough of rater variation, and thus requires additional terms (patching, cracking, etc.) in the SI model. Measurement of these additional variables increases roughness measurement time. A second problem with slope variance is that it is difficult to relate or picture physically. Because of these problems, additional research was conducted to find other pavement characterization statistics.

Power spectral or amplitude spectral estimates were one set of statistics which was investigated and, although still not considered ideal, these characterization statistics were found to be better predictor variables than slope variances. An SI model was developed based on these estimates. Extensive field testing and usage proved the usefulness of this model and it was accepted as the standard SI measurement model. Correlations between this standard and the Mays Road Meter (MRM) were made, and calibration procedures based on this model were established for all MRM's purchased for estimating SI. The correlation study is discussed in Research Report 156-1, "A Correlation Study of the Mays Road Meter with the Surface Dynamics Profilometer" (Ref 10).

This report discusses investigations into the use of power spectral or amplitude estimates as pavement characterization statistics and the development of the SI model based on these variables. Further insight into the problems of slope variance are discussed in Chapter 2. In Chapter 3, the

spectral estimates of the rating sessions from Ref 5 are examined as a means of pavement characterization. Chapter 4 discusses the development and uses of the serviceability index model based on these estimates. Finally, Chapter 5 briefly discusses the uses of digital filtering as another method for characterizing pavements.

Appendix 1 includes details of the computational methods employed in obtaining the spectral estimates. In addition, the computational details of the MRM-SI calibration program which were not included in Research Report 156-1, are given in Appendix 2.

CHAPTER 2. THE USE OF SLOPE VARIANCE FOR HIGHWAY CHARACTERIZATION

As noted in Chapter 1, initial serviceability index models were developed using slope variance and condition survey information as the independent or predictor variables.

Several disadvantages of the uses of slope variance as a pavement characterization statistic or prediction variable of pavement serviceability have been noted. First, slope variance as computed for these models has been observed to be quite dependent on wheel bounce (Refs 7 and 9). Consequently, considerable variation in replication measurements for various combinations of pavement roughness and profilometer operating speeds is common. Second, the complexity of a section of pavement cannot be adequately characterized by a single statistic such as slope variance. In addition, slope variance is difficult, if not impossible, to relate or picture physically. Finally, probably due to a large extent to the above items, slope variance alone was found to provide at best a correlation coefficient of about 0.82 and this for profilometer operating speeds of 20 mph (at greater operating speeds, this correlation dropped significantly). That is, only about 67 percent of the mean rating panel's opinion could be explained by slope variance. Roughness index was found to be similarly disadvantaged by these problems, as well as to exhibit less correlation with PSR. Adequate SI prediction models were obtained only after both condition survey information and slope variance were included. Further insight into the problems of slope variance can be gained by investigating its filter response or effect on road profile wavelengths.

As previously defined, slope variance is the variation of the slopes of a road profile. Since any such function can be expressed as a linear combination of sine and cosine terms, the filter response of slope variance or a slope variance density function can be derived as follows.

Consider a simple sine wave function of amplitude A and period T. The slope at any given point along this function is then

$$\text{Slope} = \frac{\Delta a}{\Delta t}$$

where

$$\Delta t = t_2 - t_1 ,$$

$$\Delta a = A \sin W_T(t + b) - A \sin W_T t ,$$

$$W_T = \frac{2\pi}{T} ,$$

b, base length, $= \Delta t$.

$$\therefore \quad \text{slope} = \frac{A[\sin W_T(t + b) - \sin W_T t]}{b} \tag{2.1}$$

The second moment of this then provides the power at each period T or

$$F(T) = \frac{1}{T} \int_o^T [f(x)^2]dx$$

or, thus, the slope variance for a wavelength of period T is

$$SV_T = \frac{A^2}{Tb^2} \int_o^T (\sin W_T(t + b) - \sin W_T t)^2 dt \tag{2.2}$$

$$= \frac{A^2}{Tb^2} \int_o^T (\sin^2 W_T(t + b) + \sin^2 W_T t$$

$$- 2 \sin W_T(t + b) \sin W_T t) \, dt \tag{2.3}$$

Integrating and simplifying Eq 2.3 gives

$$SV_T = \frac{A^2}{b^2} (1 - \cos W_T b) \tag{2.4}$$

which is the slope variance of a sine function for a period T and base length b . This equation is somewhat intuitive in that the slope variance for a time

series function will be zero when the base length is equal to integer multiples of the wavelength, as obviously the slopes between successive points in these cases are zero; hence its variation is zero. On the other hand, one can expect a maximum value when successive points lie at the positive and negative peaks. By assuming a unity wavelength amplitude for all wavelengths, the frequency response of slope variance can be obtained as illustrated in Fig 2.1. In this figure (note that the abscissa is represented in cycles per foot; i.e., distance is substituted for time), the function is shown for a base length of 0.75 feet, as used in the SI prediction models (Refs 5 and 9). The usefulness of slope variance as a pavement roughness indicator can be noted in this figure by its effects on long and short-wavelength profiles. For example, hills are always much larger in amplitude than bumps; however, they are not as important to riding quality as the shorter wavelength bumps or swells. Thus, the desired effect of stressing or weighing more heavily the shorter wavelength amplitudes over the longer wavelength amplitudes is obtained. On the other hand, however, the multivalued characteristics of this function could be detrimental. Since the amplitudes of the extremely high-frequency or short-wavelength bumps are very small, judicious selection of the slope base length can help minimize this effect. Figure 2.2 illustrates this response for both frequency (in cycles per foot) and base length. Analysis shows bounce occurs near 0.645 cycles and its harmonics, which is near the maximum point. Consequently, the extreme sensitivity of slope variance to profilometer operating speeds and profile roughness which was found to be common during profile measuring operations can be explained.

Because of the complexities of a road profile, pavement section wavelength components appear to be much better for the characterization of a pavement than a single statistic such as slope variance. With wavelength information, various problems such as wheel bounce can be isolated or accounted for to provide more accurate pavement characterizations.

It would also appear that at least as good a and probably a better predictor of riding quality could be obtained by correlating the effects of individual frequencies with PSR through multiple regression analysis techniques, since by this method only those frequencies which are found highly correlated could be included and the rest would be discarded.

In Chapters 3 and 4, the use of spectral estimates for characterizing highways are discussed.

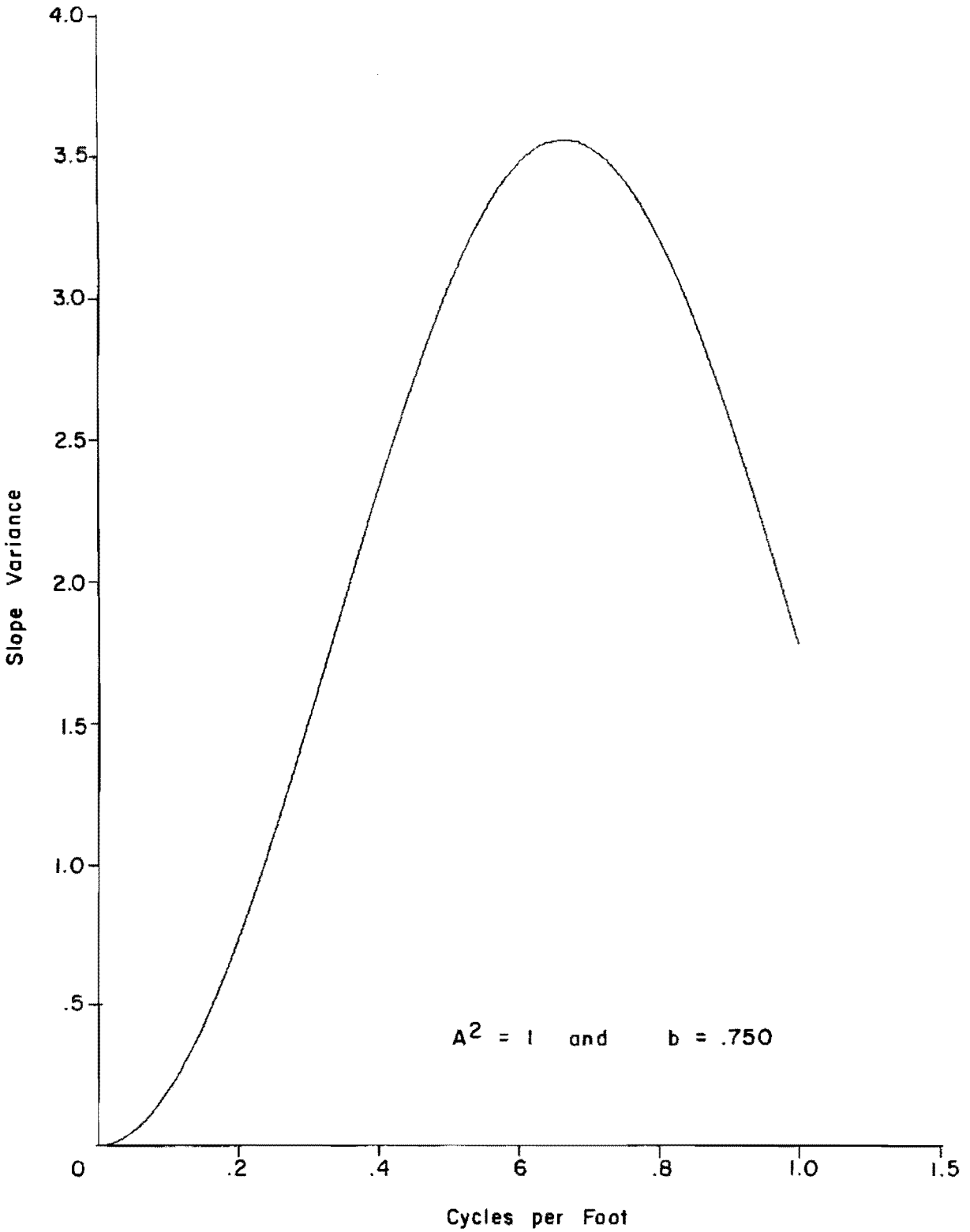

Fig 2.1. Frequency response of slope variance.

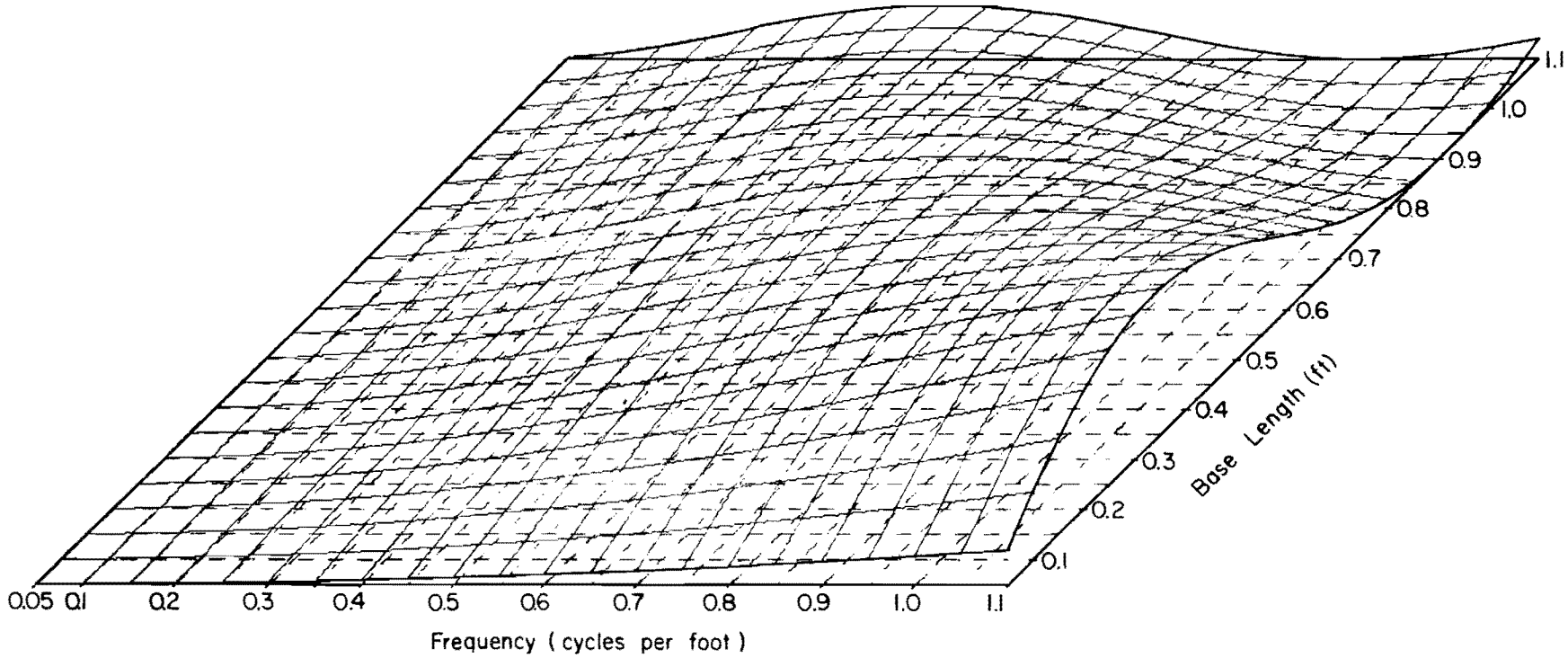

Fig 2.2. Frequency response of slope variance as function of base length.

CHAPTER 3. THE USE OF ROAD PROFILE AMPLITUDE ESTIMATES FOR HIGHWAY CHARACTERIZATION

Definitions

The term spectral analysis, as it is employed herein, includes all techniques for summarizing time series functions by separating these functions into their frequency components. A detailed discussion of spectral analysis techniques, such as Fourier transformations, power spectrum, and coherence, is not included, but information on these analysis tools can readily be found in the literature. However, a brief definition of these terms is given here.*

The autocovariance of a function $x(t)$ at lag λ may be given as

$$C(\lambda) = \lim_{T \to \infty} \frac{1}{T} \int_{-\frac{T}{2}}^{\frac{T}{2}} x(t) \cdot x(t + \lambda)dt \tag{3.1}$$

The power spectrum is the Fourier transform of the autocovariance function, or

$$P(f) = \int_{-\infty}^{\infty} C(\lambda) \cdot e^{-i2\pi f\lambda} d\lambda \tag{3.2}$$

From the above interpretation, it can be seen that a power spectrum, so commonly used in communications engineering, geophysics, and other sciences, can also be referred to as a covariance spectrum (Ref 9). Thus, $P(f)df$ represents the contribution to the variance of the road profile waveform from frequencies f and $(f + df)$. A power spectrum, therefore, is another

---

* See Ref 9 for a discussion of the assumptions necessary for computing spectral estimates of road profile data obtained with the SD Profilometer.

statistic, like slope variance, except that it provides a set of spectral values or variance densities for a road profile section whereas slope variance or simple variance yields only one such value. It is this fact which prompted an interest in the investigation of spectral analysis as a means of providing some measure of roadway roughness.

Information on energy differences between two or more time series can be obtained with cross-spectrum analysis. Whereas the power spectrum is the Fourier transform of the autocovariance, the cross-power spectrum is the Fourier transform of the crosscovariance function between two separate time signals.

It is sometimes helpful to talk about the amplitude spectrum of a section of road profile rather than its power or covariance spectrum. Such estimates are usually more easily visualized physically by the highway engineer than are, say, the power spectrum estimates; i.e., the root-mean-square amplitude of the profile irregularities in, say, inches is more easily understood than power in, say, $in.^2/(cycle/ft)$. Such amplitudes may be obtained from the power spectral estimates from

$$x_i = \sqrt{2Q_i \Delta f}$$

where Q_i represents the two-sided power or covariance spectrum component for the i^{th} frequency band and Δf is the frequency containing this variance.

Investigating Spectral Estimates of Rating Session Data

In order to investigate the usefulness of spectral estimates for characterizing a pavement, the original rating session data (Ref 5) were reexamined using 86 nonrepeated representative test sections in the Houston and Dallas-Fort Worth areas. The power or variance spectral estimates of each of the road profiles of these 1200-foot sections were then obtained as described in the Appendix. For these estimates, the spectrum was first broken into 32 bands yielding approximately 52 degrees of freedom for the spectral estimates and then into 64 bands (26 degrees of freedom). For each profile section, the power spectral estimates for the right and left wheel paths and the cross-power were all computed. Figures 3.1 and 3.2 depict typical digitized road

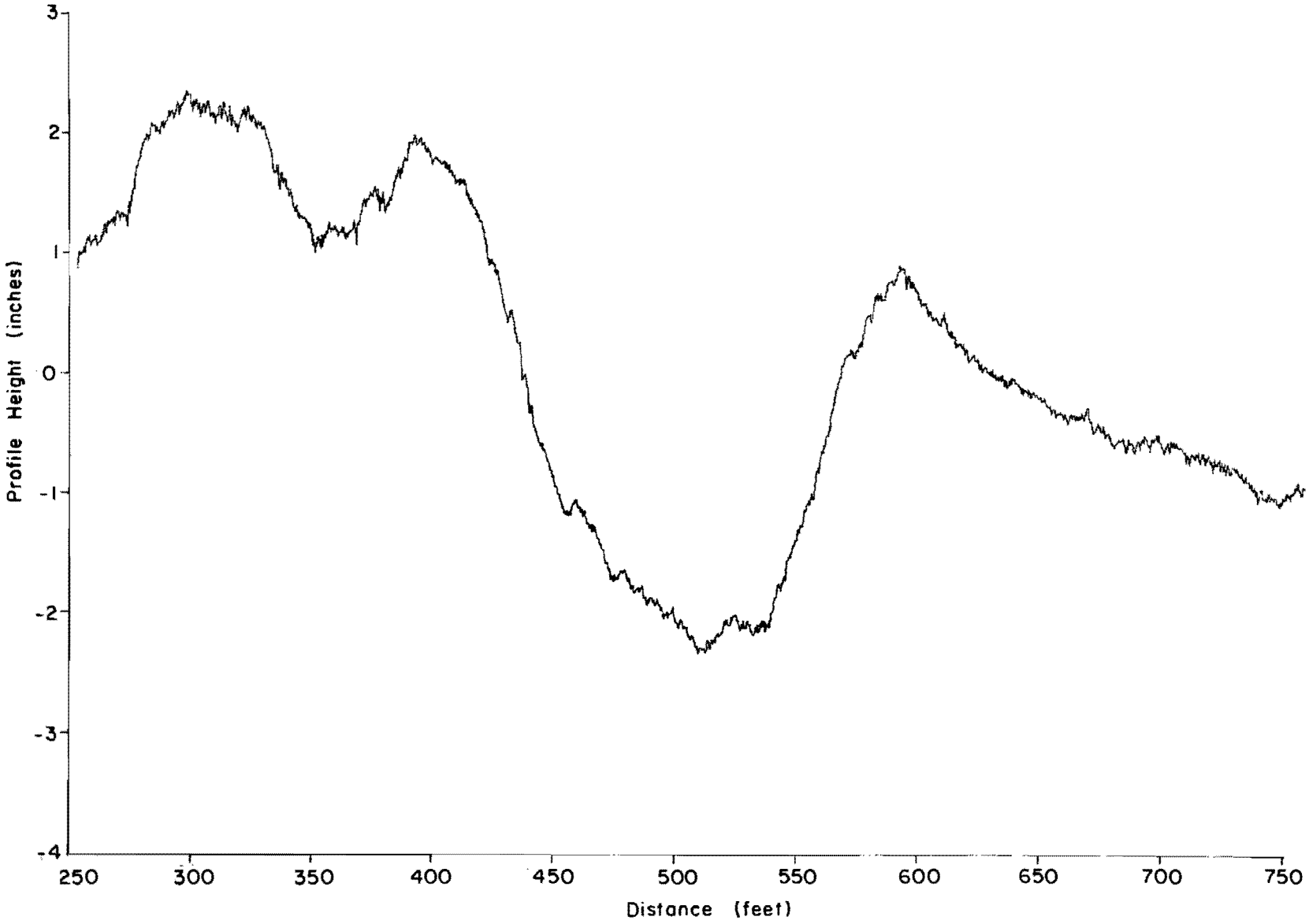

Fig 3.1. Road profile data - left wheel path.

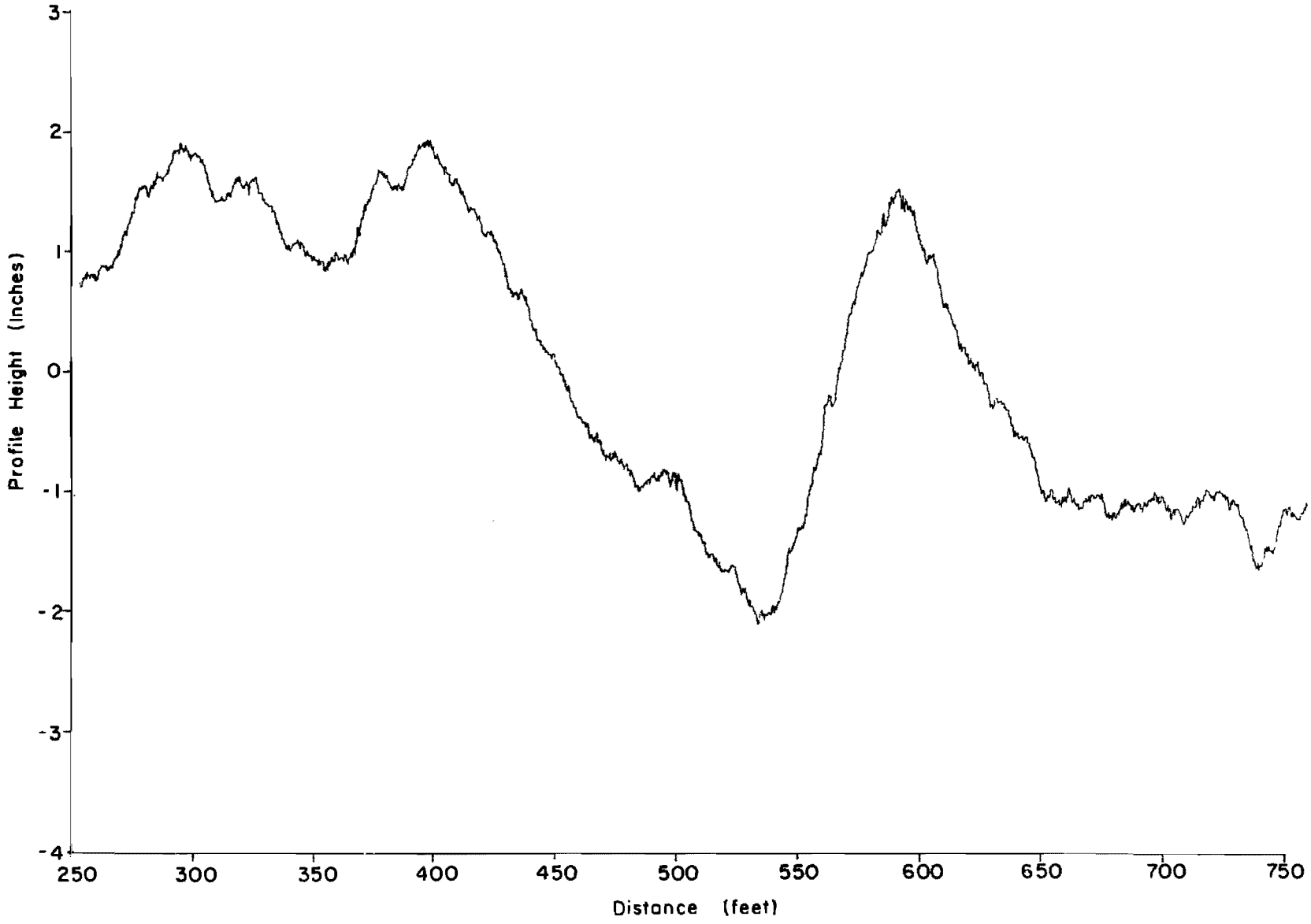

Fig 3.2. Road profile data - right wheel path.

profile plots for the right and left wheel paths. Figures 3.3 and 3.4 illustrate typical right and left power spectral plots that were computed for all 87 profile sections. As noted from the power spectral plots, the higher-frequency components are filtered. From previous observations, validated in the run-to-run coherence estimates of Ref 9, the high-frequency components generally are not of interest. Thus, to reduce the already rather extreme computation requirements, the data were decimated.

Figures 3.5 and 3.6 illustrate the relationships between the mean subjective rating panel measurement, PSR, and the road profile spectral estimates for the first ten bands of the 32-band and 64-band data. For these figures, the power spectral estimates for several frequencies or wavelength bands are shown for various road roughness classes, as indicated by PSR. That is, the 86 pavement sections covering the gamut of pavement roughness were grouped as shown (PSR intervals from 4.5 to 5.0, 4.0 to 4.5, etc.) and their average spectral amplitudes were obtained. As noted in this figure, in general, the rougher the road the greater the spectral amplitudes. However, as also may be noted for the higher frequencies or smaller wavelengths, these groupings are less discriminating as roughness indicators.

Table 1 provides a summary of these estimates for the various road classes for the same PSR intervals. For each frequency band of these two intervals, the mean power and a corresponding approximate upper 3σ amplitude range are provided. The upper range for the individual amplitude term is also provided, since it might be useful in construction control studies; i.e., typically mean amplitude values should not exceed these upper ranges (control of such specifications is, of course, another matter). For example, roads in Texas are typically designed to allow deviations from a 10-foot straightedge to be no greater than 1/8 inch. As noted, roads in the roughness class of 2.5 to 3.0 (frequency near 0.104) are near this upper range. The values in this table however, should be viewed as rough estimates, since their accuracy depends on the statistical assumptions necessary for accurate power spectrum estimates (Ref 9), which are not exactly met. Another useful analysis method would be to examine the profile data with digital filtering techniques, as described in Chapter 5. With such techniques, the amplitudes within specific frequency bands can be examined as a function of distance along the road.

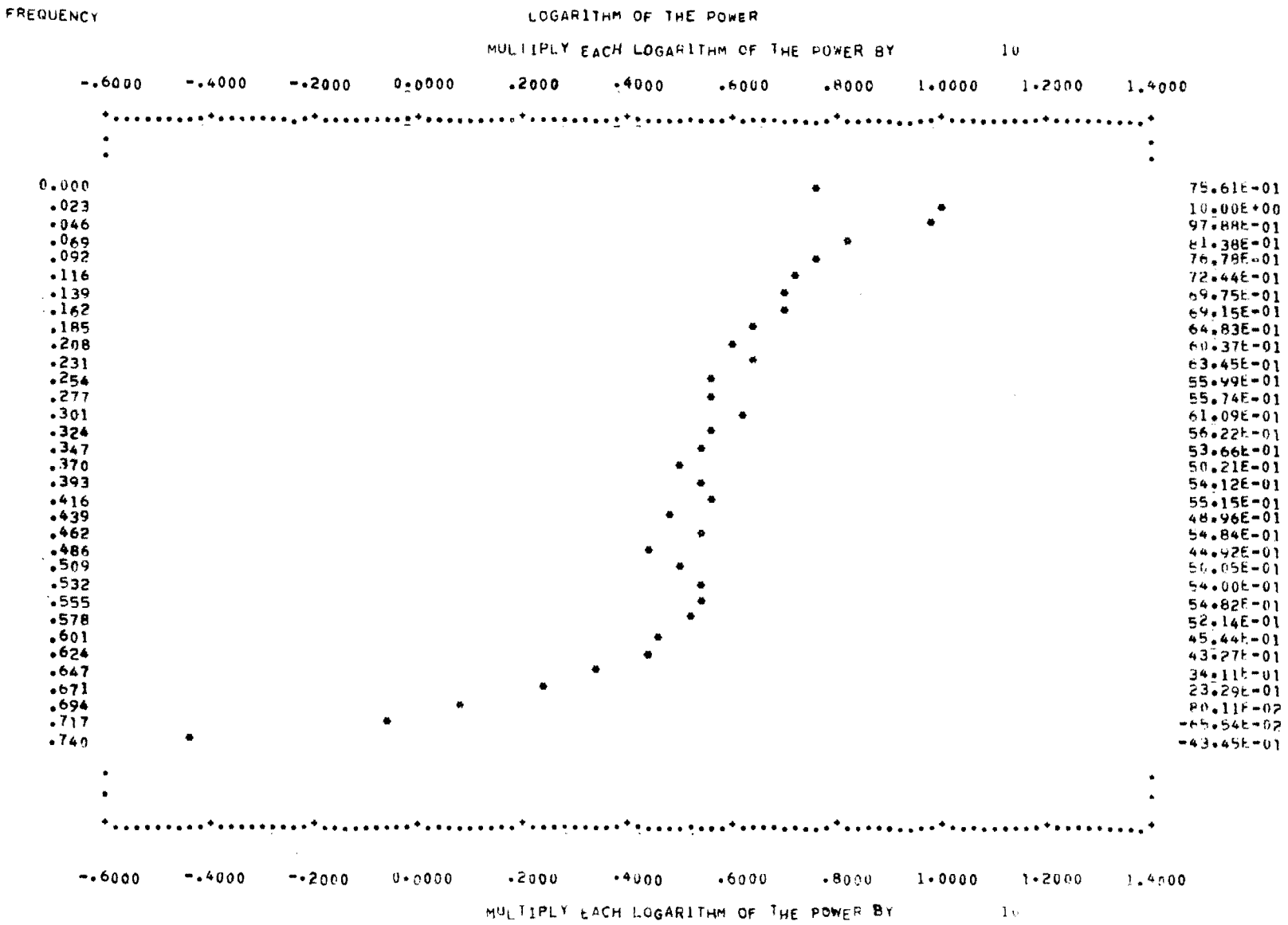

Fig 3.3. Power spectral plots - right wheel path.

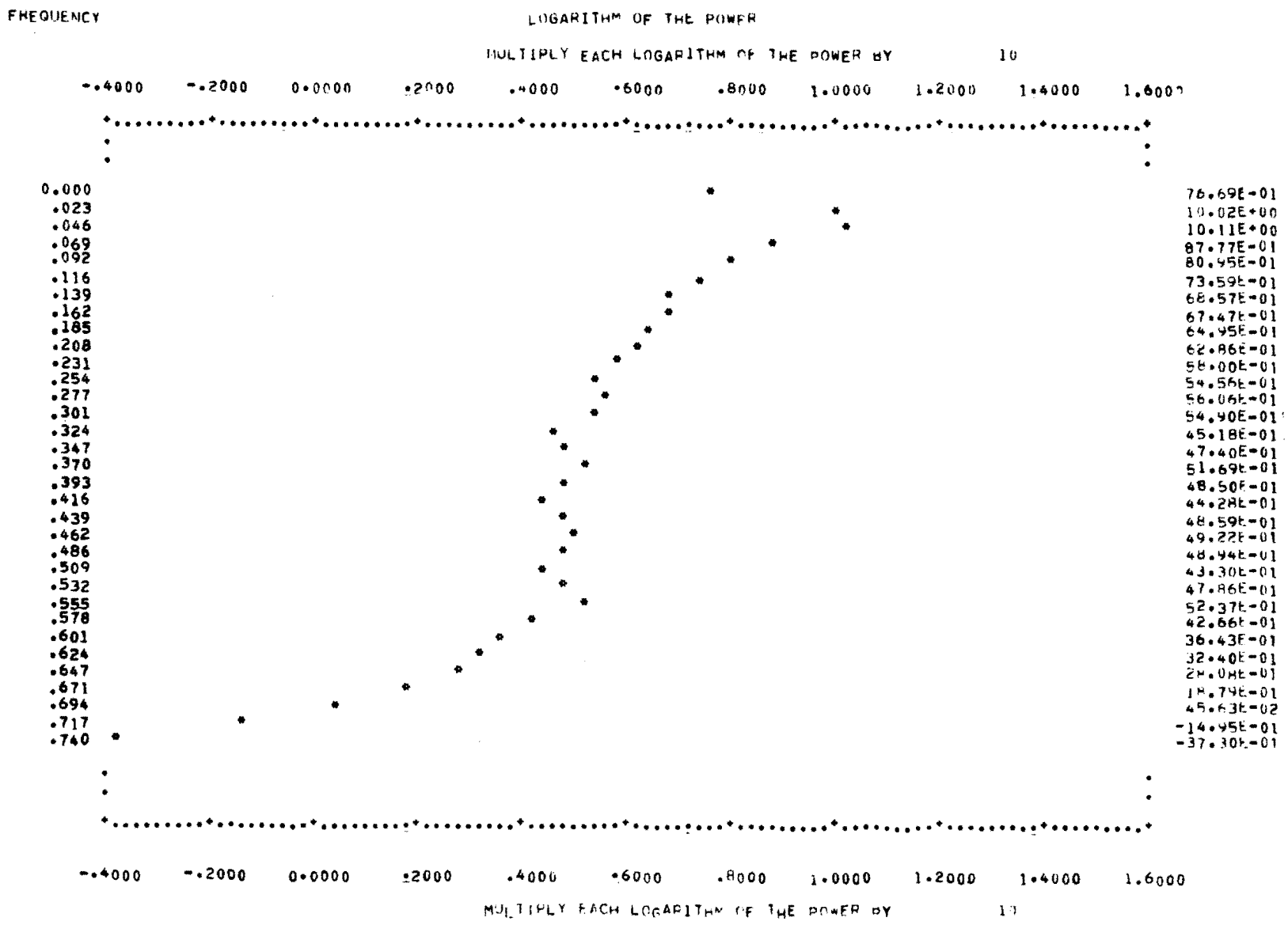

Fig 3.4. Power spectral plots - left wheel path.

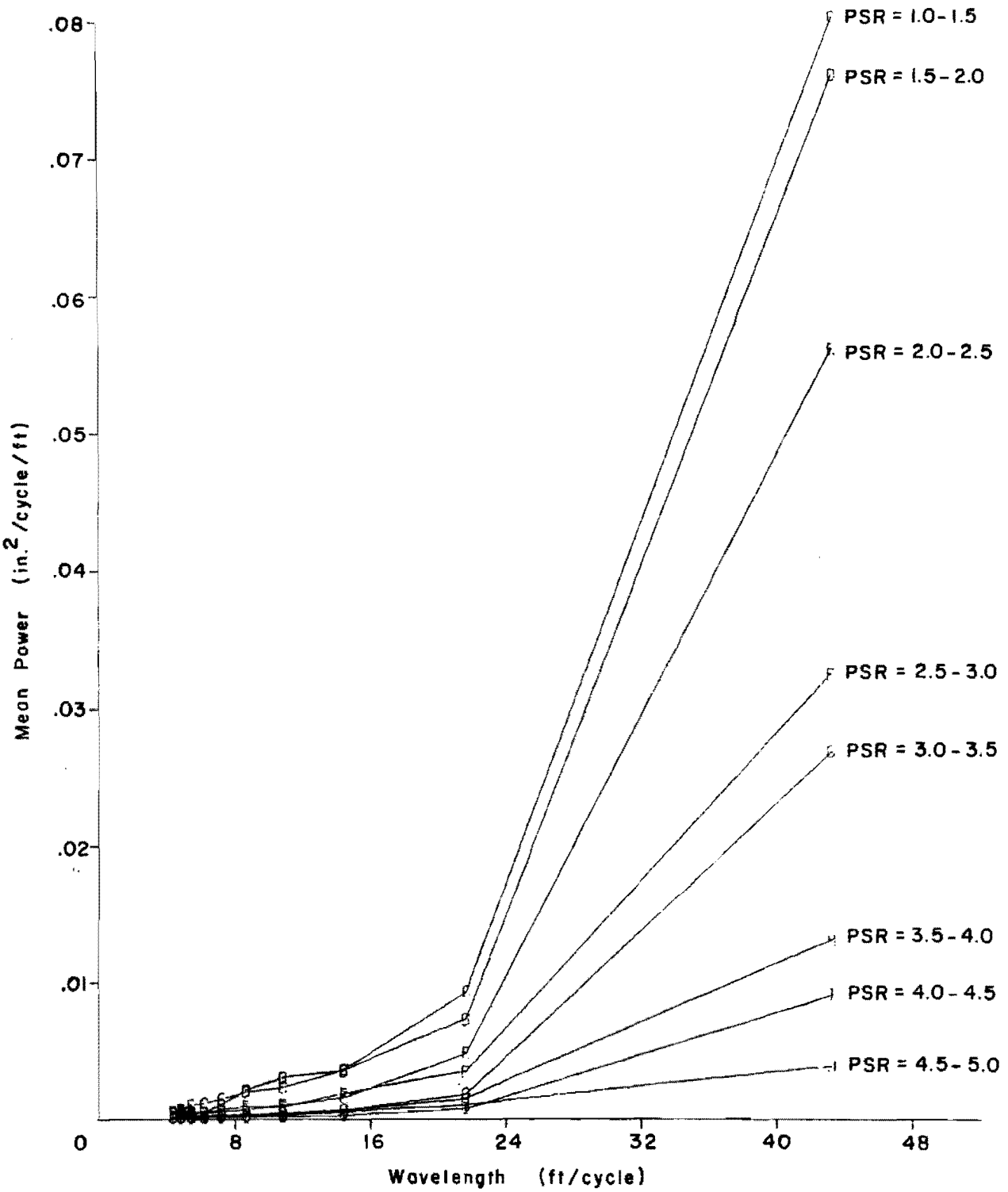

Fig 3.5. Wavelength amplitudes for rating session data.

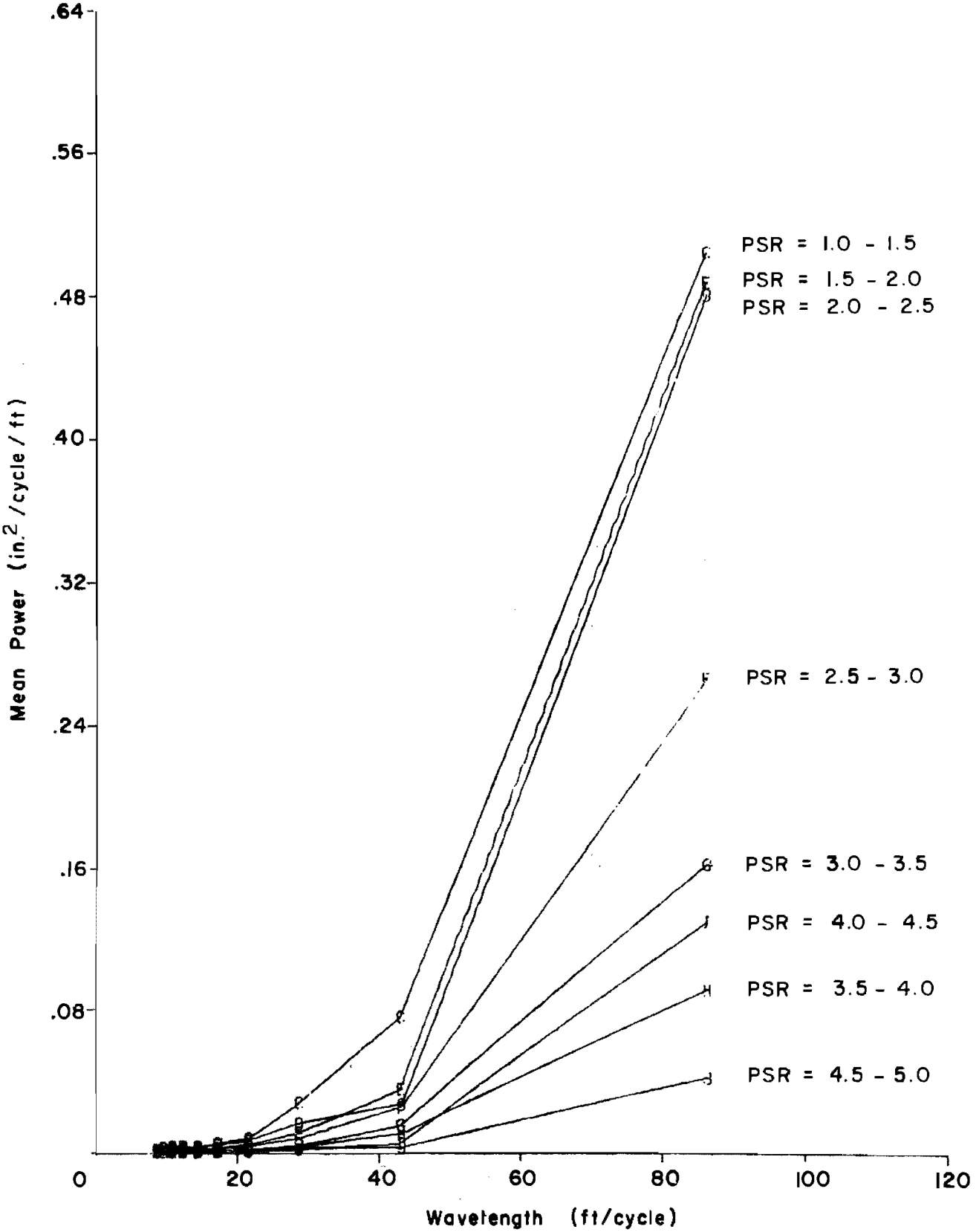

Fig 3.6. Wavelength versus power spectral estimates (64-band) for rating session data.

TABLE 1. AMPLITUDE STATISTICS FOR PSR LEVELS

Frequency (cpf)	Power Mean (in^2/cpf)	Approximate Amplitude for Upper 3σ (inches)
	PSR INTERVAL 4.0 TO 4.5 (19 SECTIONS)	
0.012	1.2945	1.4134
0.023	0.0520	0.2833
0.035	0.0159	0.1566
0.046	0.0076	0.1085
0.058	0.0044	0.0823
0.069	0.0028	0.0661
0.081	0.0025	0.0617
0.092	0.0022	0.0580
0.104	0.0018	0.0526
0.116	0.0017	0.0516
	PSR INTERVAL 2.0 TO 2.5 (10 SECTIONS)	
0.012	2.6602	2.0262
0.023	0.2538	0.6258
0.035	0.0759	0.3422
0.046	0.0307	0.2176
0.058	0.0249	0.1960
0.069	0.0174	0.1641
0.081	0.0108	0.1291
0.092	0.0087	0.1161
0.104	0.0082	0.1127
0.116	0.0084	0.1140

CHAPTER 4. SI MODEL DEVELOPMENT AND USES

Model Development

As discussed in Chapter 2, the riding quality of pavements can be subjectively established by having a group of representative highway users rate these pavements. These ratings can then be correlated to some physical characteristic of the pavement or road such as the summary statistic slope variance. As further discussed in Chapter 2, the profile wavelength components appear to be natural candidates for use as such identifying characteristics. The model could then be used for establishing, for instance, the relative importance of wavelengths present in the road.

To predict a pavement serviceability index as a function of profile wavelength, the following linear model is considered:

$$PSR = \beta_0 + \beta_1 X_1 + \beta_2 X_2 + \beta_3 X_3 + \ldots \beta_N X_N + \epsilon \qquad (4.1)$$

where

β_i = the linear model parameters, and

X_i = the average wavelength amplitudes.

Average wavelength amplitudes will be used as the independent variables, because these values are more easily visualized physically by the highway engineer than are, say, the power spectrum estimates.

To develop the model, the original rating session data described in Chapter 4 were reexamined using the mean panel ratings from 86 representative test sections throughout Texas as the dependent variable. The amplitude estimates for each of the road profiles of these 1200-foot sections were then used as the independent variables.

From Figs 3.3 and 3.4, it appears that there should be some appropriate equation which relates SI to power spectrum estimates and thus wave amplitudes.

The problem is to determine which wavelengths or bands to include in such a function or model.

A stepwise regression procedure was used with the PSR values from the original rating session experiment as the dependent variables and the logs of the wavelength amplitudes as the independent variables. Regression analysis assumes that the dependent variable is the only random variable. Since there are errors in these independent variables and these errors are not symmetrically distributed (power spectrum or variance estimates are distributed according to the chi-square distribution), they tend to bias the results unless these errors are symmetrically distributed. Thus, the log transformation on these values was used.* In addition, the independent variables were centered before the regression was performed.

Initially, the stepwise regression procedure was performed on the 32-band model where 90 independent variables, the first 30 wavelength bands for the right, left, and cross-amplitudes, were used. The regression procedure stopped after some 42 variables of the possible 90 had been included. Upon examining the standard error of residuals for each step, however, it was noted that this error reduces to about 0.198 and then begins fluctuating. The multiple correlation coefficient R^2 for this step was 0.96. However, a model should also make sense physically. Upon examining the correlation matrix of the independent variables with the dependent variables, it was noted that the right and left amplitudes (or power spectral estimates) were negatively correlated with PSR. This is plausible and illustrated in Figs 3.3 and 3.4; i.e., the greater the power the rougher the ride. However, when the regression models were examined, some of the coefficients for these same amplitudes were found to be positive, implying the greater their amplitude the better the performance — a direct contradiction. The high correlation of some of the wavelength components with the performance index indicates that these variables should be used in a model.

Average right and left amplitudes in conjunction with cross-amplitudes were next considered. The same type of results once again occurred. However, this time more negative coefficients were brought into the model. Since the

---

* It should be noted that after performing the log transformation, only a constant separates the power spectral amplitudes from the profile wave amplitudes. Thus, similar results can be obtained using power spectral estimates as the independent variables, rather than wave amplitudes.

adjacent power spectral estimates for the high frequencies (0.23 cpf and higher) are very highly correlated and since these frequencies are not very well correlated to PSR, it was decided to use the ten most highly correlated (with PSR) right and left average variables and all possible combinations of the second-order interactions concomitant with the cross-amplitude terms. The result of the stepwise regression procedure in this case provided a much more realistic function. Equation 4.2 provides the results of this regression.

$$\begin{aligned} SI = {} & 3.24 - 1.47X_1 - 0.133X_2 \\ & - 0.54X_3 + 1.08XC_1 - 0.25XC_2 \\ & + 0.08X_2X_3 - 0.91X_3X_4 + 0.67X_6X_{10} \\ & + 0.49T \end{aligned} \tag{4.2}$$

where

$X_1 = \log A_{0.023} + 2.881$

$X_2 = \log A_{0.046} + 4.065$

$X_3 = \log A_{0.069} + 4.544$

$X_4 = \log A_{0.093} + 4.811$

$X_6 = \log A_{0.139} + 5.113$

$X_{10} = \log A_{0.231} + 5.467$

$XC_1 = \log C_{0.023} + 3.053$

$XC_5 = \log C_{0.116} + 5.659$

A_i = average right and left wave length amplitude, in inches;

C_i = cross-amplitude, in inches;

i = frequency band, in cycles per foot;

T = 1 for rigid pavements and 0 for flexible pavements.

Table 2 lists the results of the regression procedure.

In an attempt to obtain a better model, the same regression procedure was rerun on 64-band power spectrum estimates (32 degrees of freedom for each estimate) of the same data. The multiple correlation coefficient (R^2) for the model in this case increased to 0.89 and the standard error of residual decreased to 0.33; however, more interaction terms entered the model. The 64-band model is as follows:

$$\begin{aligned} SI = {} & 3.41 - 1.43X_1 - .306X_2 - .180X_4 - .644X_5 + 1.25C_1 \\ & - .458X_2^2 - 1.05X_4^2 - 0.986X_5^2 + .841X_7^2 + 1.76X_1X_4 \\ & - 1.35X_1X_6 - 1.06X_1X_8 - 1.84X_1X_9 + 2.16X_1X_{10} \\ & + 1.21X_2X_5 + .741X_4X_9 + 1.51X_5X_7 - 1.65X_5X_{10} \\ & - 2.03X_7X_8 + 1.81X_8X_{10} + .679T \end{aligned} \tag{4.3}$$

where

$$X_1 = \log A_{0.012} - .426$$

$$X_2 = \log A_{0.023} + 0.895$$

$$X_3 = \log A_{0.035} + 1.481$$

$$X_4 = \log A_{0.046} + 1.893$$

$$X_5 = \log A_{0.058} + 2.139$$

$$X_6 = \log A_{0.069} + 2.351$$

$$X_7 = \log A_{0.081} + 2.500$$

$$X_8 = \log A_{0.092} + 2.593$$

$$X_9 = \log A_{0.104} + 2.670$$

$$X_{10} = \log A_{0.116} + 2.744$$

$$C_1 = \log CP_{0.012} - .3389$$

TABLE 2. REGRESSION ANALYSIS RESULTS
(32-Band Model)

Multiple correlation coefficient $R^2 = 0.81$

Standard error for residuals = 0.38

Source	DF	Sum of Squares	Mean Square	F-Ratio
Regression	9	47.68	5.297	37.46
Residual	76	10.75	0.1414	

Table 3 lists the analysis of variance of this regression. Both models were used on several test sections and essentially the same results were obtained. However, it was decided to use the 64-band model for the following reasons:

(1) Irregularities at all frequencies are usually present in a road (as indicated by Figs 3.3 and 3.4).

(2) Because of the nonorthogonality of the independent variables, these additional interaction terms should aid the prediction equation not only in fitting the original data but in field applications.

(3) All terms were found to have acceptable partial F levels.

Many other regression procedures were tried but none provided as good a model as the above. Even so, these two models are not considered ideal. Some of the problems in the modeling procedure which could have led to difficulties that prevented obtaining a more desirable SI model are discussed here.

First, the linear scale rating method that was used is similar to the one used at the AASHO Road Test, which has been criticized as not giving an adequate subjective representation. If not all pavement classes are properly distinguished by the raters, it becomes difficult if not impossible to obtain an appropriate model.

Second, as noted for the higher frequencies (or shorter wavelengths), adjacent power spectrum estimates are highly correlated. For the lower frequencies (or longer wavelengths), this correlation drops significantly. For example, the correlation coefficient R between the first and second bands (0.0116 and 0.0231 cycles per foot) was 0.599. For bands above 0.231, these values increased to above 0.9. These upper frequencies, however, were not found to be very highly correlated with PSR. Also, when the average amplitude levels for frequencies of 0.231 cycles per foot and higher were examined, it was noted that their values were very much less than 0.01 foot for the smoother roads, which is well beyond the measuring accuracies of the vehicle. As roads get rougher, these levels increase in the same proportion. Since these frequencies probably do affect roughness for some of the rougher classes of roads, a better technique should be used for including their effect in the equation. Because of their high interrelationships and their unreliability for the smooth roads, these values were omitted. Even though the long wavelength components are not as highly correlated among each other, they are correlated which leads to difficulty in obtaining an ideal model.

TABLE 3. REGRESSION ANALYSIS RESULTS
(64-Band Model)

Multiple correlation coefficient $R^2 = 0.89$

Standard error for residuals = 0.33

Source	DF	Sum of Squares	Mean Square	F-Ratio
Regression	21	51.49	2.451	22.57
Residual	64	6.951	0.109	

Uses of the Model

A desirable regression model should

(1) make sense physically,

(2) show suitable correlation between the dependent and independent variables,

(3) exhibit an acceptably small degree of lack-of-fit, and

(4) produce reasonable results in actual field use.

Although not ideal, these models do appear to make sense in that the greater the amplitude terms, the smaller the SI readings. The cross-amplitude term (which comes from cross-power) is a little more difficult to define physically; however, it indicates the similarities between the two profile heights (cross-roll or roughness effects). The interaction terms are useful in fitting the model.

The best practical test for the model is how well it performs in use. The performance of this model on over 500 miles of pavements has been quite acceptable and it is currently being used for all SI measurements involving the SD Profilometer. Table 4 provides a typical set of repeat data runs. That is, three different 1200-foot pavement sections (none of which was included in the original rating sessions) were each run five times with the SD Profilometer. The data were digitized and the power spectrum estimates computed for each run. The appropriate terms were then computed and the SI obtained for each run.

It should be noted that although current SI measurements involve first SDP profile measurement runs, analog-to-digital conversion, and finally the SI measurement computations by a program on the digital computer, the entire process could be performed in real-time during profilometer runs by a small onboard mini-computer such as an HP 2100. Fast Fourier transform hardware which is available on such mini-computers would provide considerable aid in such computations, thus minimizing central memory requirements to around 8,096 words. In addition to performing the SI model computation, the computer could also replace many of the functions currently being performed by the analog computer and thus make the overall SDP hardware cost about the same.

Figures 4.1 and 4.2 provide additional illustrations of the uses of the model, the first (Fig 4.1) in computing the SI frequency distribution of

TABLE 4. SI REPLICATIONS

Test	Run	SI
	1	4.50
	2	4.53
I	3	4.61
	4	4.57
	5	4.57
	1	4.18
	2	3.70
II	3	3.76
	4	3.98
	5	4.14
	1	2.02
	2	1.69
III	3	1.53
	4	1.92
	5	1.86

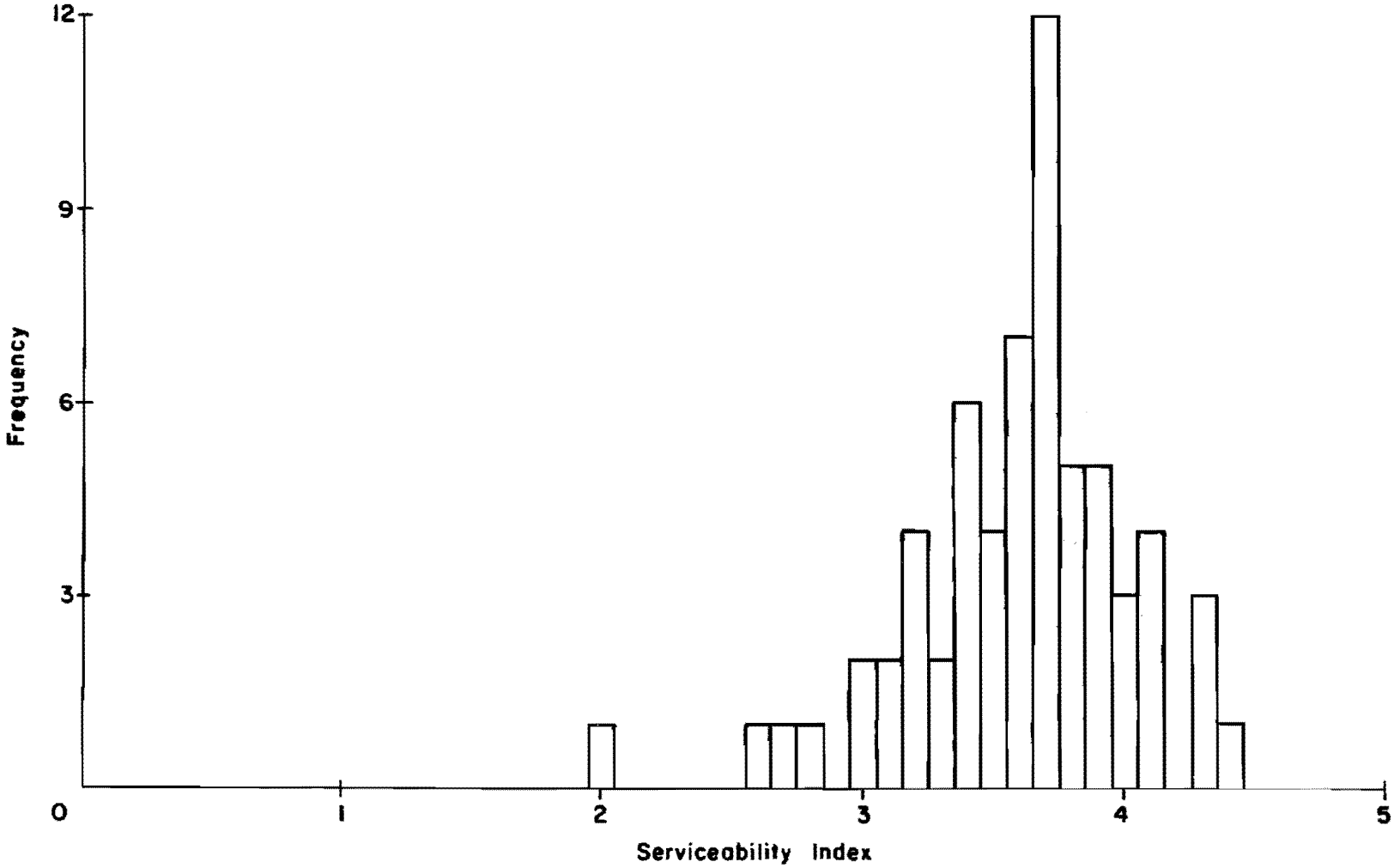

Fig 4.1. SI histogram for US 71 south of Austin.

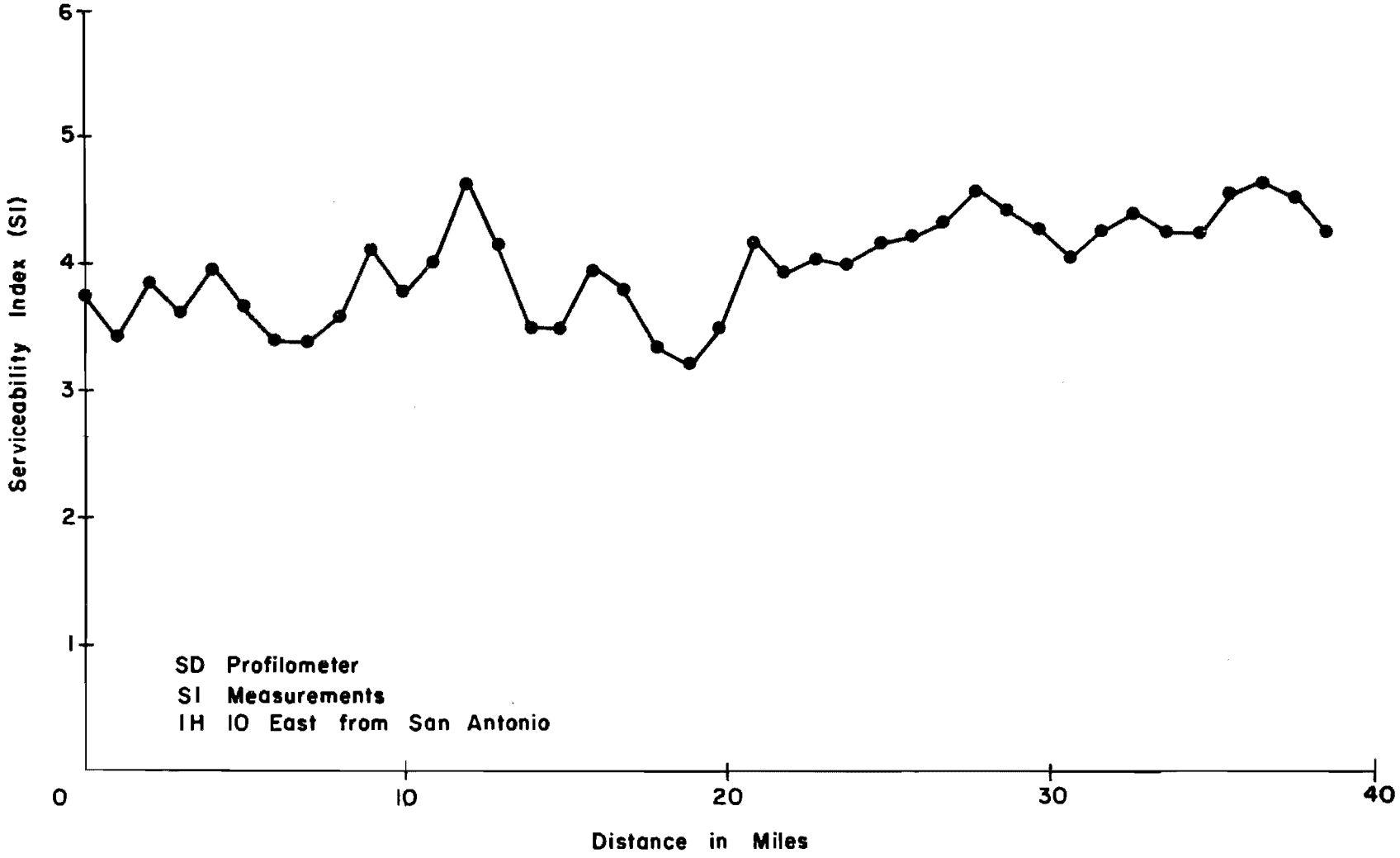

Fig 4.2. SD Profilometer SI measurements on IH 10 east of San Antonio.

several miles of pavements on US 71 south of Austin, and the second (Fig 4.2) providing SI samples for several miles of IH 10 east of San Antonio.

Because of the stability found through field use of the model, it is also currently being used for Mays Road Meter (MRM) calibrations (Ref 10). The relationship found between the Mays Road Meter cumulative roughness readings, in inches per mile, and the SD Profilometer SI measurements is

$$SI = 5e^{-\left(\frac{\log_e M}{\beta}\right)^{\alpha}} \tag{4.4}$$

where

M = the MRM roughness readings, in inches per mile; and

β and α = the MRM instrument coefficients (regression coefficients).

This equation was obtained by regressing the MRM readings onto the SI values and then solving for SI. A typical plot of this equation for one of the MRM devices calibrated to the SI standard is shown in Fig 4.3.

Other Modeling Considerations

As noted in the preceding section, even though a highly usable model was developed, an ideal SI model was not obtained. This could have been due to the rating procedure as indicated, or simply because no such model exists. Several different modeling techniques were investigated. For instance, factor analysis methods were employed and a regression performed on the orthogonalized variables. Clustering methods were also briefly investigated where some similarities between the various variables could be established and related to PSR. Tables 5 and 6 illustrate the uses of these methods for comparing groupings to PSR. For this example, four clusters were selected using the convergent k-means clustering algorithm and $\left[\sum (x_i - \bar{x})^2\right]^{1/2}$ similarity measurement for the log of the power spectral estimates of the first 10 bands (32-band data); i.e., 10 variables. Additional investigations into the uses of various clustering techniques might provide better characterizing methods.

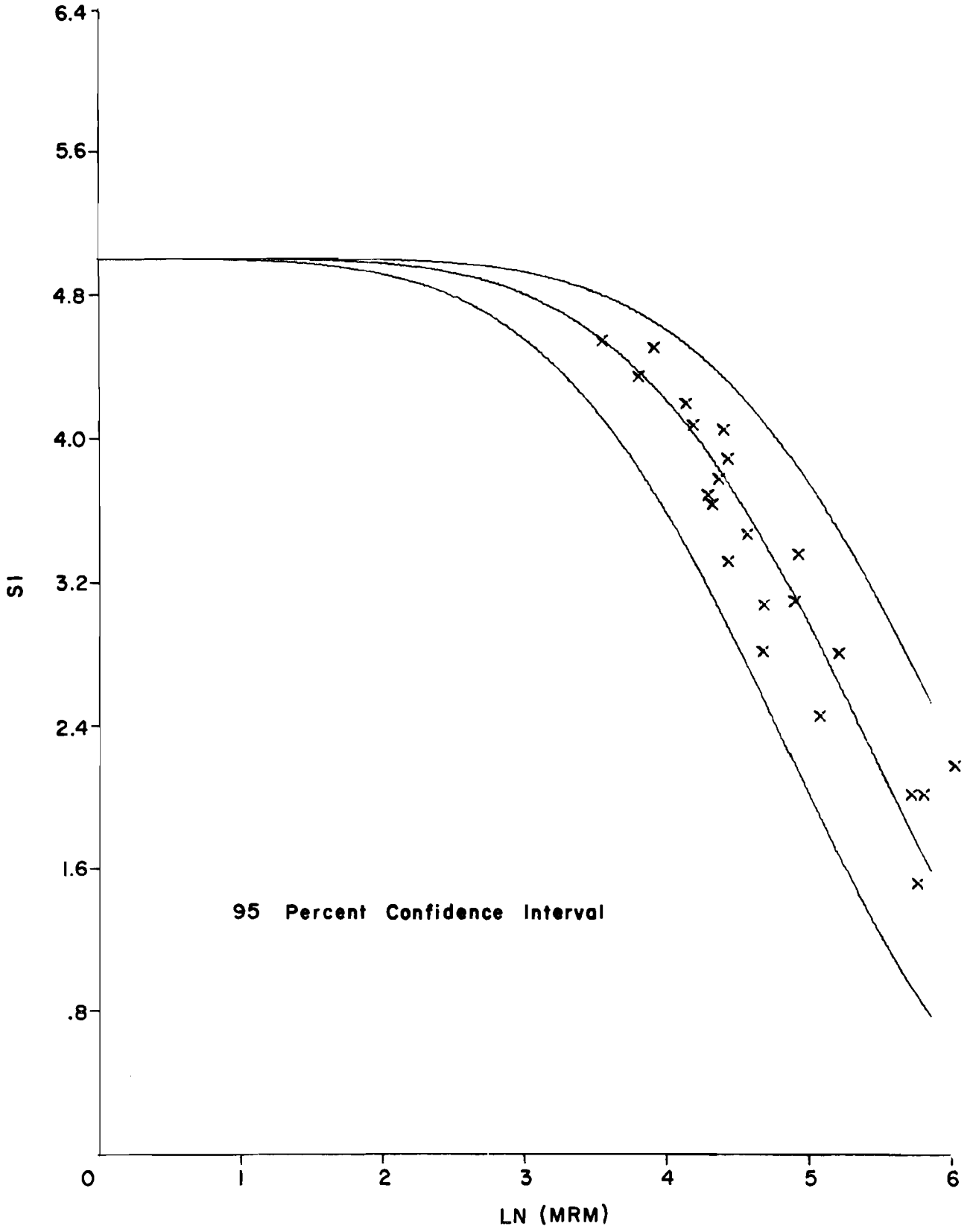

Fig 4.3. SD Profilometer SI values versus Mays Road Meter roughness readings.

TABLE 5. CLUSTER ANALYSIS - FLEXIBLE PAVEMENTS

Cluster 1	
Members (PSR)	2.1, 1.6, 1.1, 2.1, 2.1, 2.1, 2.9, 2.7
Cluster 2	
Members (PSR)	3.2, 4.2, 3.6, 2.9, 3.6, 2.4, 3.1, 3.3, 3.8, 2.4, 3.9, 3.7, 3.0, 3.2, 3.7, 3.7, 3.8, 3.7, 4.0, 4.2, 3.6, 3.9, 1.1, 3.8, 3.5
Cluster 3	
Members (PSR)	4.3, 4.0, 4.4, 4.1, 4.1, 3.9, 4.3, 4.0, 3.9, 3.6, 4.3
Cluster 4	
Members (PSR)	2.1, 1.5, 3.4, 3.4, 2.1, 3.2, 3.3, 3.9, 4.0, 3.5, 2.5, 2.7, 4.1

TABLE 6. CLUSTER ANALYSIS - RIGID PAVEMENTS

Cluster 1	
Members (PSR)	3.2, 2.1, 2.9, 3.4, 2.1, 3.6, 2.1, 2.4, 2.1, 2.4, 3.3, 3.9, 3.7, 3.9, 1.1, 2.7
Cluster 2	
Members (PSR)	4.2, 3.6, 3.1, 3.3, 3.8, 3.7, 3.0, 3.2, 3.7, 3.8, 3.7, 4.0, 3.6, 3.8, 3.5
Cluster 3	
Members (PSR)	4.3, 4.0, 4.4, 4.1, 4.1, 3.9, 4.3, 4.0, 3.9, 3.9, 3.6, 4.3, 4.2
Cluster 4	
Members (PSR)	2.1, 1.5, 1.6, 1.1, 3.4, 2.1, 3.2, 2.9, 4.0, 3.5, 2.5, 2.7, 4.1

CHAPTER 5. THE USE OF DIGITAL FILTERING FOR ROAD PROFILE ANALYSIS

Introduction

There are several problems in using power spectral analysis methods in analyzing road profile signals, the primary problem being that the spectral estimates obtained are a mean amplitude estimate for each particular band. Assuming that the profile data meet the usual statistical assumptions (gaussian, stationary, ergodic, etc.) and enough samples are present, this mean is a good estimate of the real profile amplitude from which a good indication of the characteristics of the individual time or distance ensembles can be obtained. On the other hand, however, if these assumptions are not met, which is usually the case, then the amplitude estimates can become distorted. Filtering techniques offer another analysis tool in which the amplitudes of selected wavelength bands can be observed as a function of distance, thus permitting more localized examinations of the true average amplitude variations. Digital filtering methods are attractive for such analysis techniques for analyzing road profile data because of the analog-to-digital and digital computing facilities available at the Center for Highway Research and the Texas Highway Department. For this reason, this chapter will briefly provide some of the general definitions for such filtering methods, illustrate some initial uses of these methods, and discuss possible future applications. References are provided in which more details of these methods can be obtained.

Digital Filtering Definitions

Digital filtering is the process of spectrum shaping using a digital computer as the basic building block (Ref 2). Hence, the goals of digital filtering are similar to those of continuous or analog filtering. Whereas continuous filter theory is based on linear differential equations, digital filter theory is based on linear difference equations.

Digital filters are usually applied to discrete time series (such as digitized road profile data) by convolving the input series with the weighing

function (impulse response) of the filter (see Fig 5.1). The convolution is designed as follows:

$$y_n = \sum_{i=0}^{N} w_i x_{n-i} \tag{5.1}$$

where

X = $\{x_0, x_1, \ldots x_M\}$ represent $M + 1$ values of the input series or road profile

W = $\{w_0, w_1, \ldots w_N\}$ represent $N + 1$ values of the filter weighing function

Y = $\{y_0, y_1, \ldots y_{N+M}\}$ represent the $N + M + 1$ values of the filtered output series

Equation 5.1 can also be expressed in terms of its z transform as

$$Y(z) = W(z)\, X(z) \tag{5.2}$$

where

$$X(z) = x_0 + x_1 z + x_2 z^2 + \ldots x_M z^M$$
$$W(z) = w_0 + w_1 z + w_2 z^2 + \ldots w_N z^N$$
$$Y(z) = y_0 + y_1 z + y_2 z^2 + \ldots y_{M+N} z^{M+N}$$

The variable z which represents the operation of delaying a data sample one sample interval (z^N by N sample intervals) is related to the Laplace variable S by the equation

$$z = e^{-TS} \tag{5.3}$$

where T is the Δt sample interval.

Some digital filters can also be expressed as a ratio of two polynomials in z, or

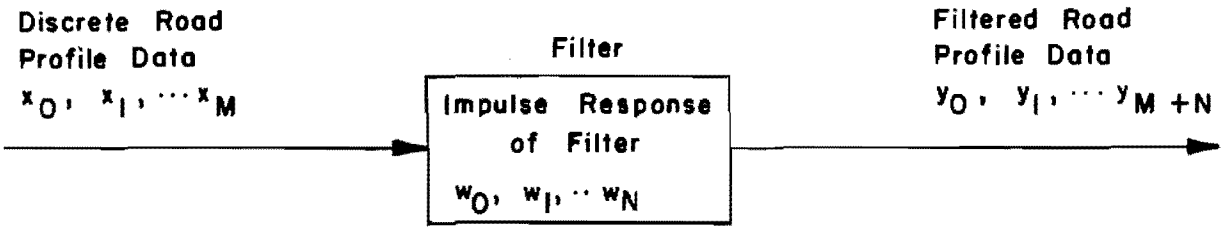

Where : $Y = WX$ Time Convolution

$Y(z) = W(z) \cdot X(z)$ Related z Transform

Fig 5.1. Digital filtering.

$$W(z) = \frac{A(z)}{B(z)} = \frac{a_0 + a_1 z + \ldots a_N z^N}{b_0 + b_1 z + \ldots b_M z^M} \tag{5.4}$$

By using long division (Ref 6) we may expand $W(z)$ into a simple polynomial:

$$\frac{A(z)}{B(z)} = w_0 + w_1 z + w_2 z^2 + \ldots \tag{5.5}$$

If the filter is stable, the coefficients will converge to zero and hence $W(z)$ may be closely approximated by a finite number of terms, say K such terms, or

$$W(z) = \frac{A(z)}{B(z)} \approx w_0 + w_1 z + \ldots w_K z^K \tag{5.6}$$

This approximation can then be used as a filter by standard digital convolution. If the rational filter

$$W(z) = \frac{a_0 + a_1 z}{1 + b_1 z + b_2 z^2} \tag{5.7}$$

is used to filter a set of profile data then the standard output $Y(z)$ can be expressed as

$$Y(z) = \frac{a_0 + a_1 z}{1 + b_1 z + b_2 z^2} \; X(z)$$

or

$$Y(z) + zY(z)\,[b_1 + b_2 z] = [a_0 + a_1 z]\, X(z)$$

and thus

$$Y(z) = [a_0 + a_1 z]\, X(z) - zY(z)\,[b_1 + b_2 z] \tag{5.8}$$

That is, Y(z) is equal to the input convolved with the series (a_0, a_1) minus the output delayed one sample interval and convolved with the series (b_1, b_2).

Figure 5.2 illustrates this feedback system which is realized by the recursive algorithm of Eq 5.8. The general recursive equation for rational filters can be expressed as

$$y_n = \sum_{i=0}^{M} a_i x_{n-i} - \sum_{j=1}^{M} b_j y_{n-j} \qquad (5.9)$$

Such filters* may be synthesized in the z plane or standard S plane filters can be converted to such recursive relationships.

Recursive filters may also be used for obtaining zero phase filters by the use of both forward and reverse recursive algorithms (see Ref 2).

Filtering Applications

As noted above one of the advantages in using digital filtering techniques for analyzing road profile data is that a plot of the filtered profile amplitude versus distance can be obtained. Statistical methods can be applied which first divide a pavement into sections according to similarities of the variances of the profile irregularities, and then obtain more realistic average and extreme amplitude estimates for road sections.

A simple band pass filter was applied to about two miles of pavements on a farm-to-market road near Bryan, Texas, near which swelling clay mounds were observed to occur in 20-foot wavelengths. In Fig 5.3, the response or gain of the filter is plotted versus frequency. The gain is the multiple by which the amplitude of an input sine wave is decreased by filtering. Note that at the filter's center frequency, .05 cpf, the gain is one; i.e., an input sine wave with frequency .05 cpf would have the same amplitude after filtering as before. The gain decreases quickly as the frequency moves away from .05 cpf, which indicates that the filter essentially removes all irregularities except those whose frequencies are near .05 cpf. Since frequency is expressed in cpf, the corresponding wavelengths are the reciprocals of the frequencies; i.e.,

---

* Refs 2, 4, and 6 should be consulted for more details of such filtering techniques.

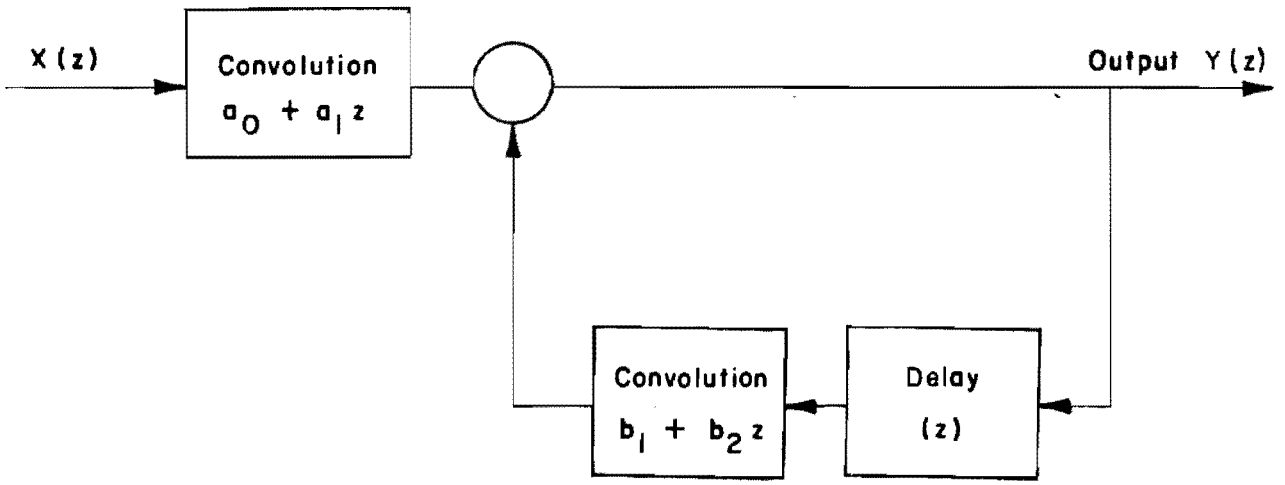

Fig 5.2. Recursive digital filter (after Ref 6).

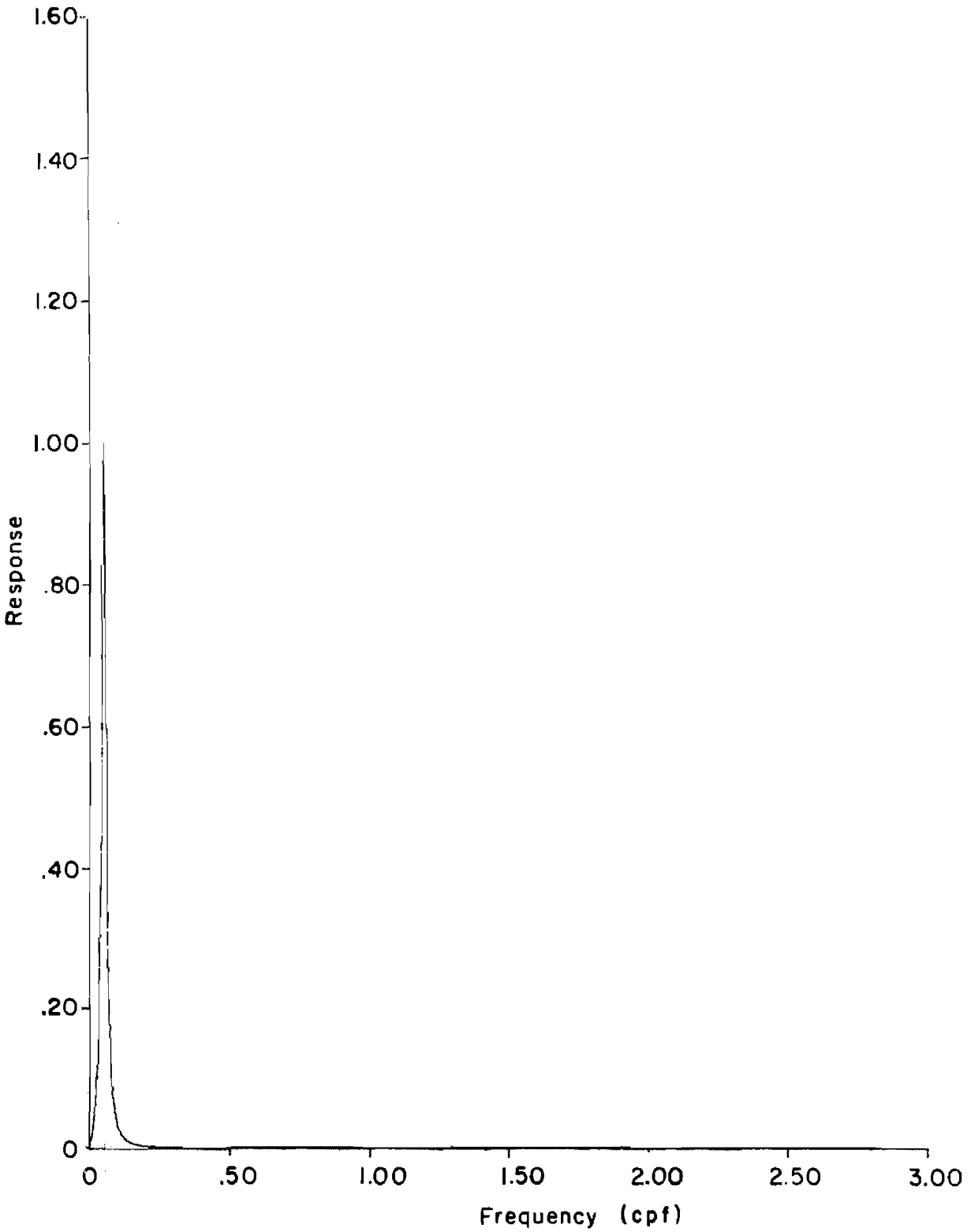

Fig 5.3. Frequency response of band pass filter of Eq 5.10.

the wavelength corresponding to .05 cpf is 1/(.05 cpf) or 20 feet per cycle. The time or impulse response of this filter is depicted in Fig 5.4. The coefficients used in obtaining this filter are given in Eq 5.10:

$$y_n = (-5.375 \times 10^{-6})x_{n-1} + (5.375 \times 10^{-6})x_{n-5} + 3.954\ y_{n-1} - 5.870\ y_{n-2} + 3.876\ y_{n-3} - 0.9610\ y_{n-4} \quad (5.10)$$

for a Nyquist frequency of 2.96 cpf.

Figures 5.5 through 5.7 show the plots of these data before and after zero phase filtering was performed. The zero phase filtering was obtained as described in Ref 2, or, after using the forward recursive algorithm of Eq 5.10, the time reverse algorithm of Eq 5.11 was applied:

$$y_n = (-5.375 \times 10^{-6})\ x_{n+1} + (5.375 \times 10^{-6})\ x_{n+5} + 3.954\ y_{n+1} - 5.870\ y_{n+2} + 3.876\ y_{n+3} + 0.9610\ y_{n+4} \quad (5.11)$$

One useful method of applying these filtering methods would be to establish a set of typical upper amplitude levels for construction specifications and control rather than a single number, such as 1/8 inch for 10-foot wavelengths. For example, a representative sampling of profiles from pavements of highly acceptable riding quality could be measured. Band pass filters* could be designed and used on these data to obtain several sets of filtered profile data. Mean and upper amplitude ranges (say three standard errors) could be established for appropriate roughness regions for each band of this data to establish a set or spectrum of not-to-exceed-amplitude regions (see Fig 5.8). If the mean of the absolute values of the profile elevation deviations at any wavelength exceeded the established threshold value, then the pavement would be judged unacceptable. Initially, filters centered at the bands used in the SI model of Chapter 4 might be used. Once such ranges are established, the SD Profilometer could be used for evaluation of new or recently overlayed

---

* Nonrecursive filters using the fast Fourier transform for convolution (Ref 2) might be more desirable, particularly if similarities between these filters and the amplitude estimates of Chapter 3 are to be investigated.

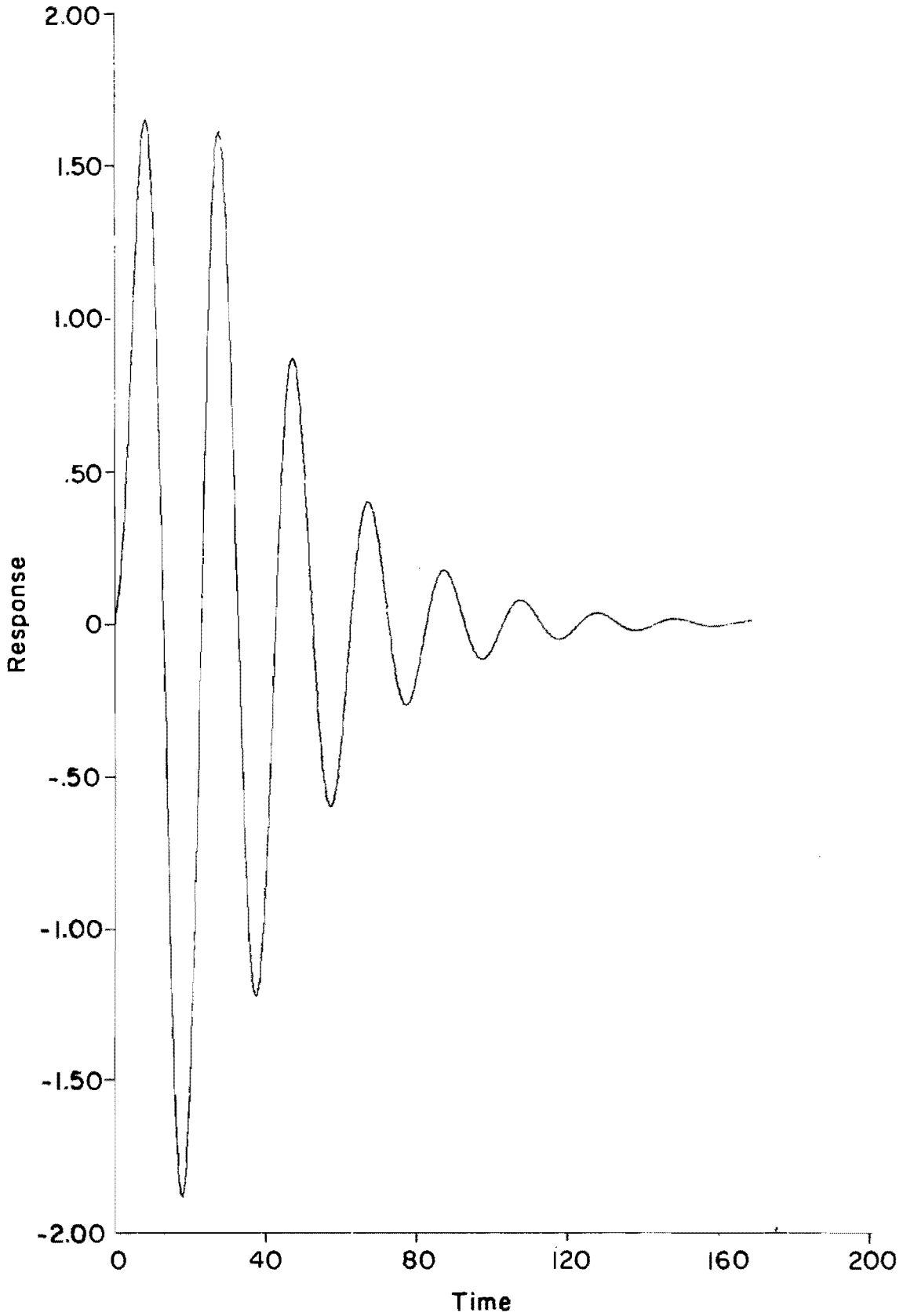

Fig 5.4. Filter impulse response.

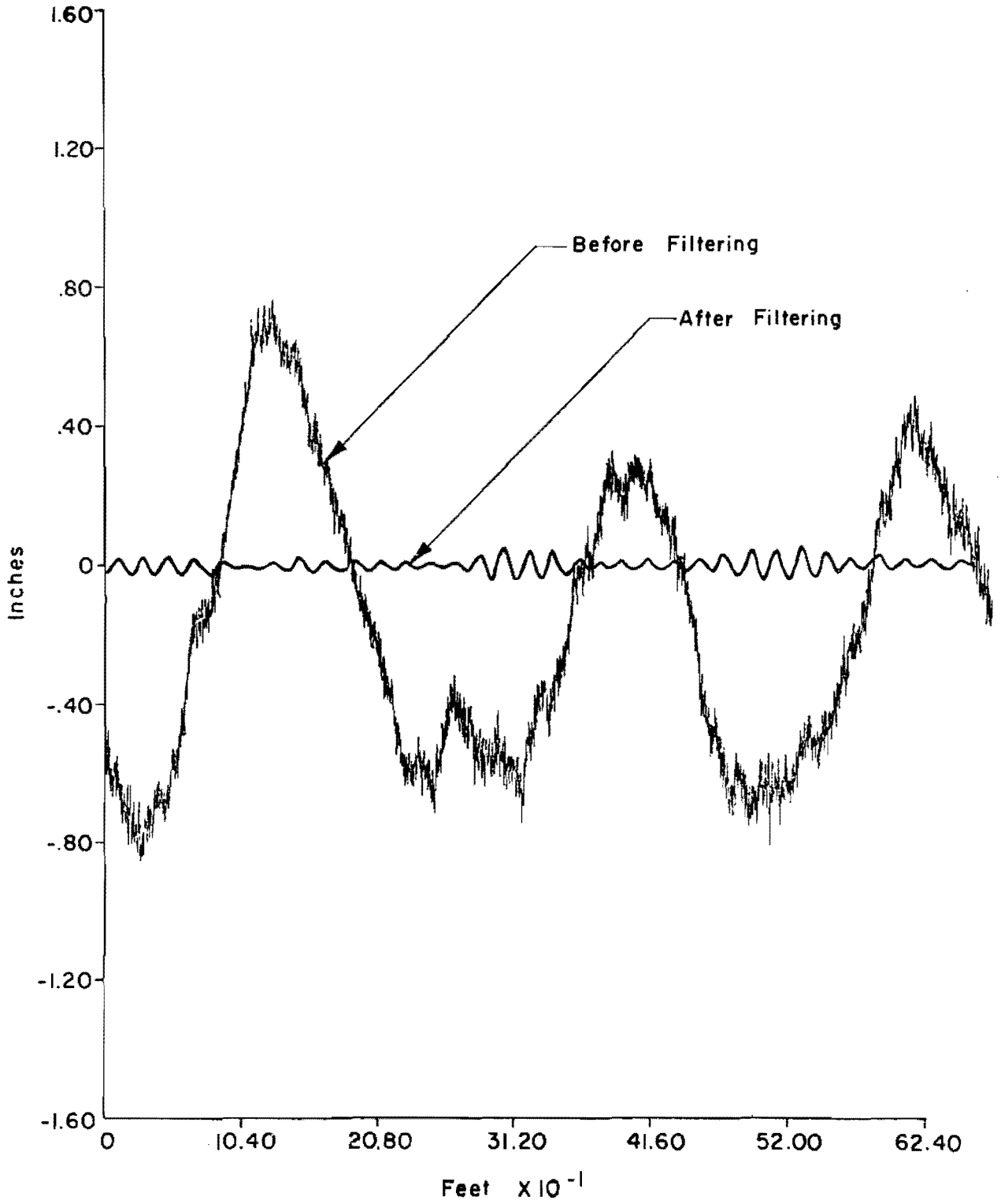

Fig 5.5. Profile before and after filtering, 0-670 feet.

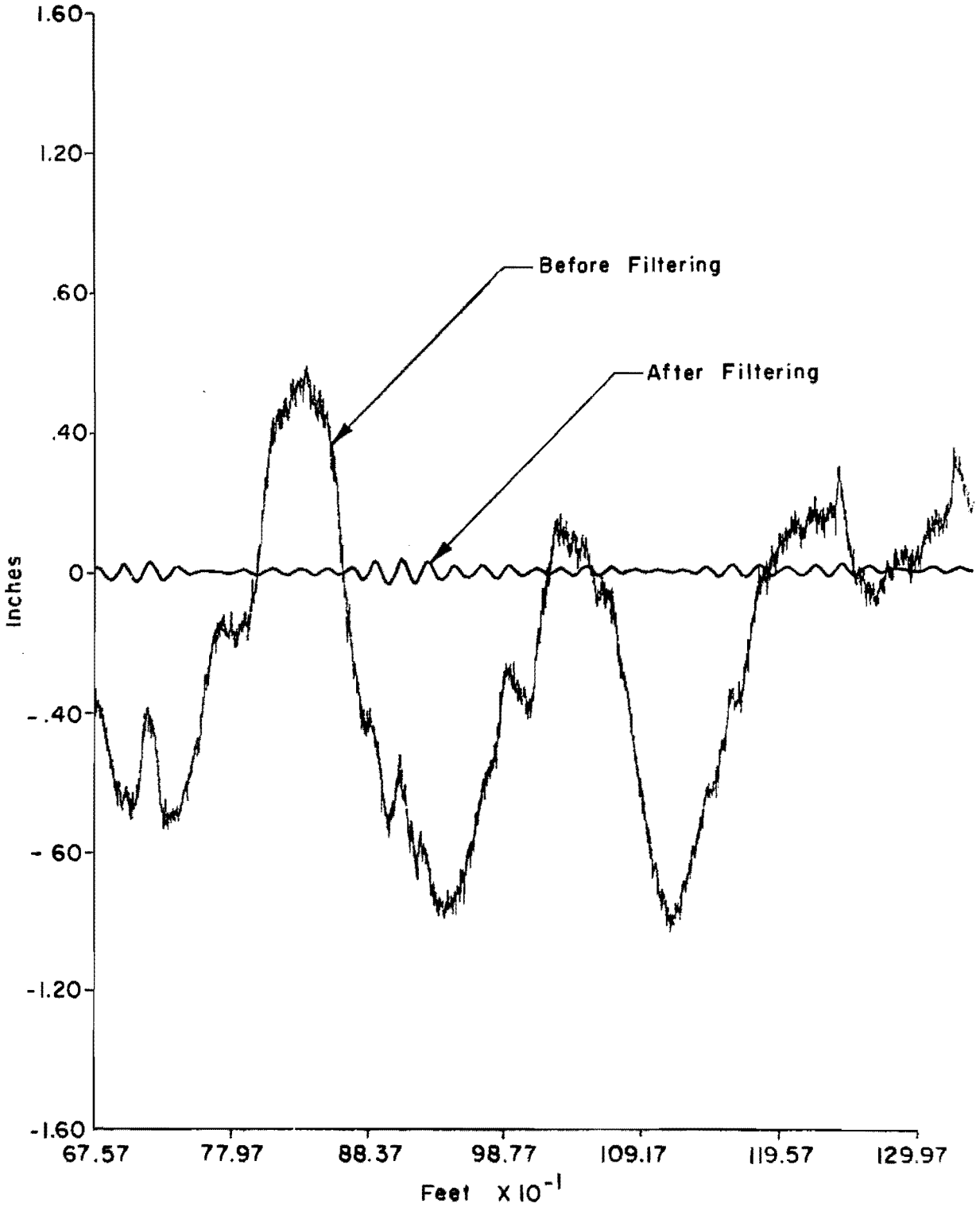

Fig 5.6. Profile before and after filtering, 670-1350 feet.

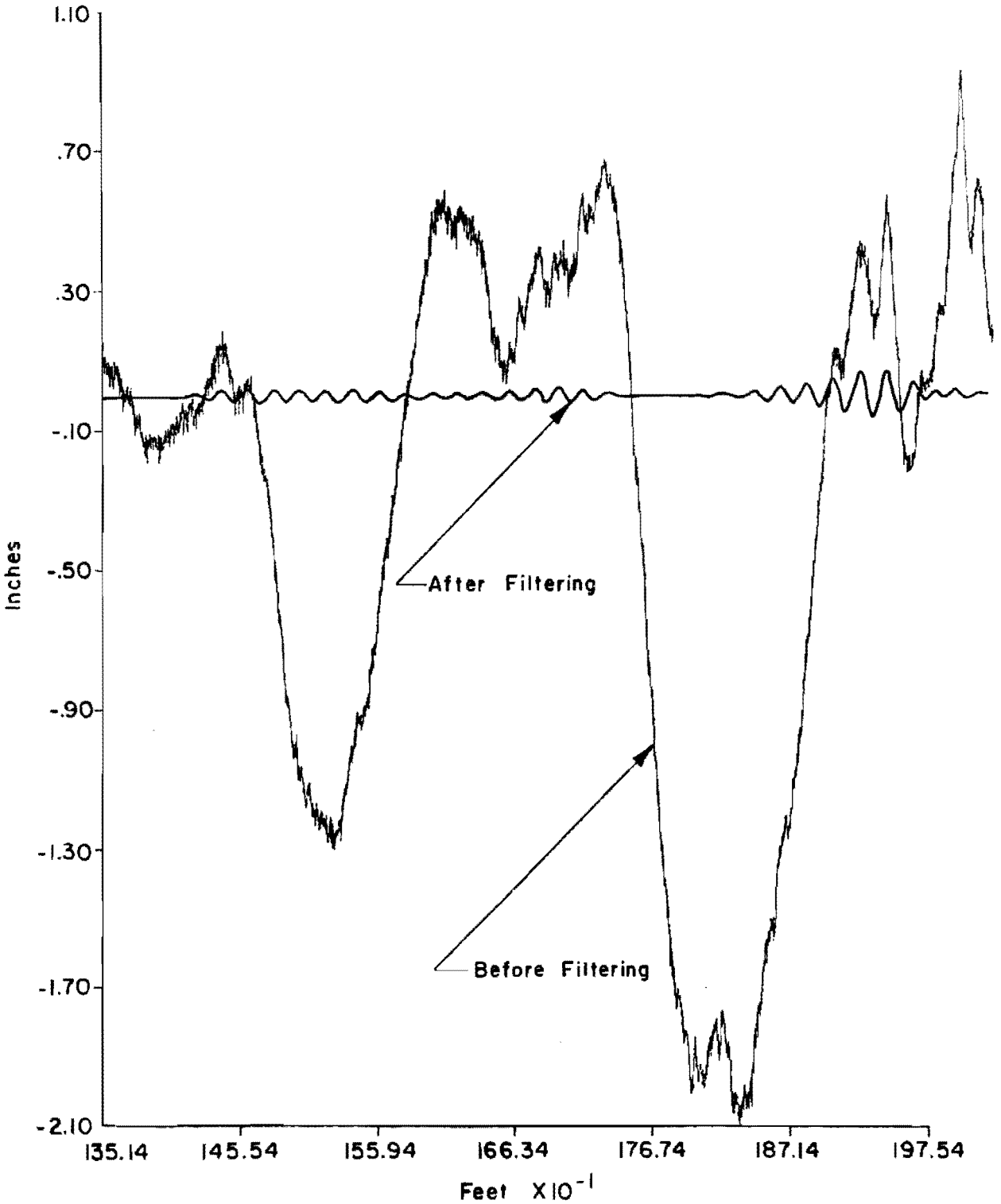

Fig 5.7. Profile before and after filtering, 1350-2000 feet.

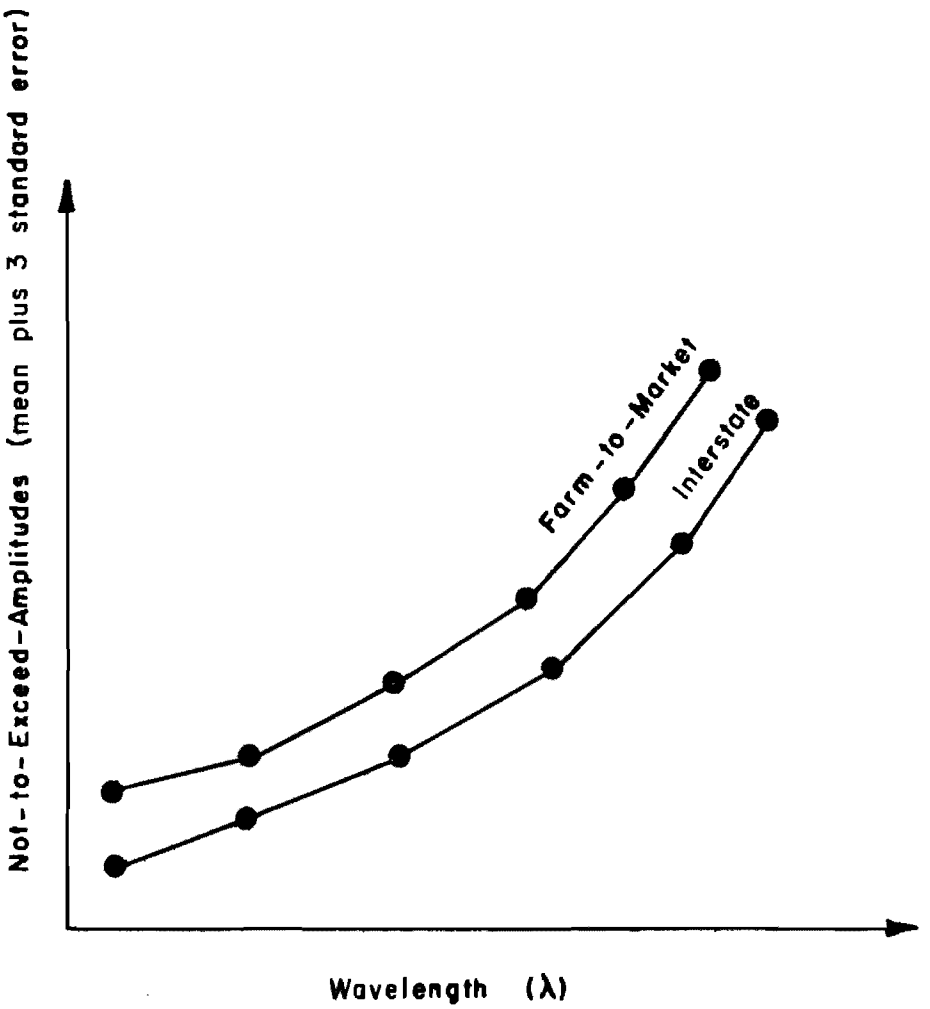

Fig 5.8. Example of not-to-exceed-amplitude levels for construction specifications.

pavements to rapidly find areas violating these critical regions. A small digital controller within the SD Profilometer could be used to easily detect such violations immediately during profile measurements.

REFERENCES

1. Carey, W. N., Jr., and P. E. Irick, "The Pavement Serviceability-Performance Concept," Bulletin 250, Highway Research Board, Washington, D. C., 1960.

2. Gold, Bernard, and Charles Rader, Digital Processing of Signals, McGraw-Hill Book Co., 1969.

3. Jenkins, Gwilym M., and Donald G. Watts, Spectral Analysis and Its Applications, Holdin-Day, 1969.

4. Rader, Charles M., and Bernard Gold, "Digital Filter Design Techniques," Technical Note 1965-63, Lincoln Laboratory, Massachusetts Institute of Technology, Lexington, December 1965.

5. Roberts, Freddy L., and W. Ronald Hudson, "Pavement Serviceability Equations Using the Surface Dynamics Profilometer," Research Report 73-3, Center for Highway Research, The University of Texas at Austin, April 1970.

6. Shanks, John L., "Recursion Filters for Digital Processing," Geophysics, Vol XXXII, No. 1, February 1967.

7. Walker, Roger S., Freddy L. Roberts, and W. Ronald Hudson, "A Profile Measuring, Recording, and Processing System," Research Report 73-2, Center for Highway Research, The University of Texas at Austin, April 1970.

8. Walker, Roger S., and W. Ronald Hudson, "Analog-to-Digital System," Research Report 73-4, Center for Highway Research, The University of Texas at Austin, April 1970.

9. Walker, Roger S., W. Ronald Hudson, and Freddy L. Roberts, "Development of a System for High-Speed Measurement of Pavement Roughness, Final Report," Research Report 73-5F, Center for Highway Research, The University of Texas at Austin, May 1971.

10. Walker, Roger S., and W. Ronald Hudson, "A Correlation Study of the Mays Road Meter with the Surface Dynamics Profilometer," Research Report 156-1, Center for Highway Research, The University of Texas at Austin, February 1973.

11. Walker, Roger S., "The Application of Some Statistical Procedures for Analyzing Spectral Data," Ph.D. Dissertation, The University of Texas at Austin, Austin, Texas, August 1972.

12. BMD Biomedical Computer Programs, University of California Publication in Automatic Computations, University of California Press, 1970.

13. Blackman, R. B., and J. W. Tukey, The Measurement of Power Spectra, Dover Publications, Inc., New York, 1958.

14. Eveleigh, Virgil W., Adaptive Control and Optimization Techniques, McGraw-Hill, 1967.

APPENDIX 1

COMPUTATIONAL METHODS

APPENDIX 1. COMPUTATIONAL METHODS

This appendix describes the computational methods used in the computer programs for computing power spectral and coherence estimates.

Computation of Power Spectral and Coherence Estimates

Power spectral and coherence estimates for the text were computed in accordance with the following six steps:

(1) data collection and A-to-D operations,
(2) data decimation and filtering,
(3) data detrending,
(4) data windowing,
(5) power spectral computations, and
(6) coherence computations.

Data Collection and A-to-D Operations. A typical road profile data collection procedure involves using the SD Profilometer for obtaining analog voltage levels proportional to the road profile of the section being measured.* This profile signal is recorded on an FM recorder along with a distance pulse providing 11.87 pulses for each foot traveled. The recorded profile data are then digitized in accordance with the distance signal, thus providing 5.93 samples per foot for both the right and left profile signals. These digitized values can be scaled to inches by dividing by a numerical value corresponding to 1 inch of road profile displacement. The scaled right and left profile data sets will be referred to respectfully as

$$[X] = x_1, x_2, \cdots x_N$$

$$[Y] = y_1, y_2, \cdots y_N$$

---

* See Refs 8 and 9 for details on the measuring system and A-to-D operations.

where the number of samples N is equal to the total section length (in feet) times 5.93 data points per foot.

Because of the upper-frequency response characteristics of the measuring system, the highest frequency present in these data will always be less than three cycles per foot, thus satisfying the sampling theorem.

Data Decimation and Filtering. Since long data sections (N data points) can become quite large and because typically the sampling resolution provided is not needed, the digitized data records are usually decimated or subsampled. Decimation usually requires low pass filtering, and thus each series is decimated and filtered by generating a new set of values as follows (Ref 12):

$$x_t = \sum_{j=-w}^{w} a_j x(t-1)d + j + w + 1$$

where

d = decimation ratio,

w = 12d (filter half-length),

$$a_j = \frac{1 + \cos(\pi M/w)}{4w} \cdot \frac{\sin[\pi(k + 1/2)j/w]}{\sin(\pi j/2w)},$$

The number of scans or data points N is then changed to

$$N = \left[\frac{N_{old} - (2w + 1)}{d}\right] + 1$$

Data Detrending. Detrending is often done in spectral analysis to help insure against nonstationarity. Reference 13 illustrates how such problems can distort the low-frequency spectral estimates. Since the SD Profilometer includes high pass filtering, such trends, if existing, are not desirable. Hence, any linear trend is removed from the two data series by replacing each data value as follows:

$$x_t = x_{old} - \bar{x} - \beta(t - \bar{t})$$

where

$$\bar{x} = \frac{1}{N} \sum_{t=1}^{N} x_t ,$$

$$\bar{t} = \frac{1}{2}(N + 1) ,$$

$$\beta = \frac{\sum_{t=1}^{N} t x_t - \frac{1}{2}N(N + 1)\bar{x}}{\frac{1}{6}N(N + 1)(2N + 1) - \frac{1}{4}N(N + 1)^2}$$

Data Windowing. To reduce the spurious side lobes which are always present in the power spectrum when the data length is finite, a cosine taper data window is applied to each data series as follows:

$$x_t = x_{old} \cdot w_t$$

where

$$w_t = \begin{cases} 0.5\{1 - \cos [\pi(t - 1/2)/r]\} & t = 1, \ldots r \\ 1 & t = r + 1, \ldots N - r \\ 0.5\{1 - \cos [\pi(N - t + 1/2)/r]\} & t = N - r + 1, \ldots N ; \end{cases}$$

$$r = [N/10]$$

The remainder of each series is then filled with zeros to a total of M^* data points.

Power Spectral Computations. The raw power spectral computations can be obtained from the discrete Fourier transform by

$$P_i = \frac{1}{F} \left(\hat{x}_i \cdot \hat{x}_i^* \right)$$

---

* M is the smallest power of 2 greater than or equal to N .

where

$\hat{x}_i$ = the Fourier transformed data array,

F = band width in hertz = frequency step size in the FFT.

For b bands, resulting in approximately N/b degrees of freedom, the power spectral terms are computed as

$$P_k = C \sum_{t=(k-1/2)d}^{(k+1/2)d} \hat{x}_t \cdot \hat{x}_t^* \qquad k = 0, \ldots b$$

where

$$d = \frac{M}{2b},$$

$$C = \frac{M}{s(d+1)} \cdot \frac{N}{N - 5/4r}$$

The term (N - 5/4r)/N is used to correct for the bias resulting from the data windowing applied in Step 4. The number d + 1 is the number of spectral estimates contained in each band computed. The frequency associated with each band is then

$$f_k = \frac{k \cdot s}{2b} \qquad k = 0, 1, \ldots b$$

As indicated above, the discrete Fourier transform is used to compute the Fourier coefficients. Since both data series are real, this transform (using the FFT algorithm) can be used for computing both series at the same time. This is possible because of the symmetrical characteristics of the transform, as indicated in Ref 3. To perform this operation, the series z is formed by placing one series, say x , in the real array and the second, y , in the imaginary array, or

$$z = x + iy$$

The Fourier transform is then made and the following relationships are used for obtaining the individual transformed values:

$$\hat{x}_t = \frac{1}{2}\left(\hat{z}_t + \hat{z}^*_{m-t}\right)$$

$$\hat{y}_t = \frac{-i}{2}\left(\hat{z}_t - \hat{z}^*_{m-t}\right)$$

Coherence Computations. Coherence computations are obtained by computing the cross-power, in the same manner as before except that both data series x and y are used, or

$$CP_k = C \sum_{t=(k-1/2)d}^{(k+1/2)d} \hat{x}_t \cdot \hat{y}^*_t \qquad k = 0, \ldots b$$

where c , d , and b are defined as before.

Coherence may then be computed as follows:

$$Coh_k = \frac{|CP_k|}{\sqrt{P_{xk} \cdot P_{yk}}}$$

The multiple regression analysis in Chapter 2 for the 32-band model illustrates the method in which a typical power spectrum analysis is set up. In this analysis, power spectral estimates were needed on 1200-foot data sections, or the maximum data series length was preset. This provides a constraint on the maximum number of bands and degrees of freedom possible. Based on these constraints, the remaining decisions made on this analysis were as follows:

Number of bands b	32
Decimation rate d	4
Number of original data scans N	6750
Sampling rate SR	5.93

From these initial specifications, the following program parameters were necessary for obtaining the spectral estimates (Steps 5 and 6):

Filter half-length = 12d = 48

Number of data points after decimation $N = \frac{6750 - 97}{4} + 1 = 1664$

New sampling rate $= \frac{s}{4} = 1.48$

Degrees of freedom $= \frac{1664}{32} = 52$

Maximum power of 2 (for FFT) = 2048

Figure A1.1 illustrates typical output provided by the program, where

Freq = frequency in cycles per foot,

P1 = power spectral estimate for right profile,

P2 = power spectral estimate for left profile,

CP = cross-power estimate,

Coh = coherence,

Phase = phase of CP and Coh .

The power and cross-power estimates shown have not been scaled (i.e., are not in inches squared per cycles per foot). The file identification indicated on the first line is used in the A-to-D and data-reduction process. That is, each profile section run was digitized and written as one data file on a seven-track magnetic tape, and the first record of each file contains the file identification shown (see Ref 8).

FILE = 6 NO. RECS. = 11 ID1 = 20 ID2 = 0

NUMBER OF SCANS BEFORE DECIMATION = 6750
NUMBER OF SCANS AFTER DECIMATION = 1664
NUMBER OF BANDS = 32 SAMPLING RATE = 1.4800

DEGREES OF FREEDOM = 52.00

FREQ	P1	P2	CP	COH	PHASE
0.0000	8.18995E+06	7.91044E+06	5.96472E+06	.74105	0.00000
.0231	2.13910E+05	9.65532E+04	6.36908E+04	.44318	69.66439
.0462	4.41240E+04	2.37911E+04	2.30415E+04	.71116	-11.91841
.0694	1.13670E+04	6.63977E+03	5.18751E+03	.59712	-15.42456
.0925	1.02487E+04	3.46121E+03	1.68610E+03	.28310	69.18076
.1156	1.31888E+04	1.48427E+03	3.31197E+02	.07486	-20.05095
.1387	1.47348E+04	1.42021E+03	2.37941E+03	.52014	157.43861
.1619	2.69887E+03	2.02654E+03	1.23245E+03	.52699	80.32638
.1850	1.73965E+03	1.09715E+03	4.85311E+02	.35128	24.04132
.2081	9.16994E+02	1.19466E+03	4.83803E+02	.44224	-44.62643
.2312	8.38166E+02	3.38947E+02	1.90668E+02	.35772	-76.90221
.2544	7.37663E+02	3.91360E+02	5.33092E+01	.09922	80.40255
.2775	9.03259E+02	3.24400E+02	3.19317E+02	.58990	.46170
.3006	3.47672E+02	4.29458E+02	1.07922E+02	.27930	109.14466
.3237	4.72333E+02	4.41065E+02	1.02067E+02	.22362	-85.40533
.3469	3.20279E+02	4.20014E+02	1.33421E+02	.36377	-83.16283
.3700	4.85713E+02	2.63381E+02	9.84599E+01	.26539	-59.13893
.3931	4.96672E+02	3.29819E+02	6.86200E+01	.16954	49.51146
.4162	3.39095E+02	5.43242E+02	2.08411E+02	.48558	-114.70868
.4394	2.89348E+02	2.24975E+02	4.20056E+01	.16464	77.16726
.4625	7.70692E+02	2.41602E+02	1.19572E+02	.27710	69.62419
.4856	8.63630E+02	3.19090E+02	9.31720E+01	.17749	-5.77466
.5087	3.26931E+02	2.59465E+02	8.65826E+01	.29728	-115.60235
.5319	1.95136E+02	1.73388E+02	6.39322E+01	.34757	-71.41284
.5550	2.44946E+02	1.07694E+02	4.48044E+01	.27586	-60.08083
.5781	1.87209E+02	1.81095E+02	2.88187E+01	.15652	105.76896
.6012	2.46518E+02	2.12605E+02	3.32302E+01	.14515	40.57634
.6244	1.73966E+02	9.91388E+01	6.57035E+01	.50030	-148.99367
.6475	9.33738E+01	2.09042E+01	2.13221E+01	.48262	142.80833
.6706	3.16625E+01	1.56267E+01	3.44328E+00	.15480	-9.38822
.6937	3.45831E+00	7.17325E+00	5.55185E-01	.11147	-162.28826
.7169	3.30416E-01	3.19348E-01	6.65248E-02	.20480	-103.50578
.7400	2.81468E-02	2.02605E-02	1.06282E-02	.44506	0.00000

Fig A1.1. Typical spectral analysis computer printout.

APPENDIX 2

MRM-SI CALIBRATION PROGRAM COMPUTATIONS

APPENDIX 2. MRM SI CALIBRATION PROGRAM COMPUTATIONS

The following calibration equation is currently being used for Mays Road Meter-SDP SI calibrations (Ref 10):

$$SI = 5e^{-\left(\frac{\ell n\ M}{\beta}\right)^{\alpha}} \qquad \text{(A2.1)}$$

This reverse regression equation is obtained by solving for SI in terms of M , the MRM roughness measurement. In the following regression equation (as described in Ref 10),

$$Y = \beta X^{1/\alpha} + \epsilon \qquad \text{(A2.2)}$$

where

$Y = \ell n\ M$;

β = regression coefficients;

M = the MRM accumulated roughness readings, in inches per mile;

$X = \ell n\,(5/SI)$;

ϵ = the residual or regression error.

the Y intercept β_o is zero; that is, the function or model passes through the origin.

A special regression procedure was developed for rapidly obtaining the α and β estimates using a self-adjusting, steepest descent, searching technique (Ref 14). Once the parameter estimates are computed the program generates the specific MRM SI calibration table as described in Ref 10. Figure A2.1 provides a flow chart of the technique used for computing the calibration table.

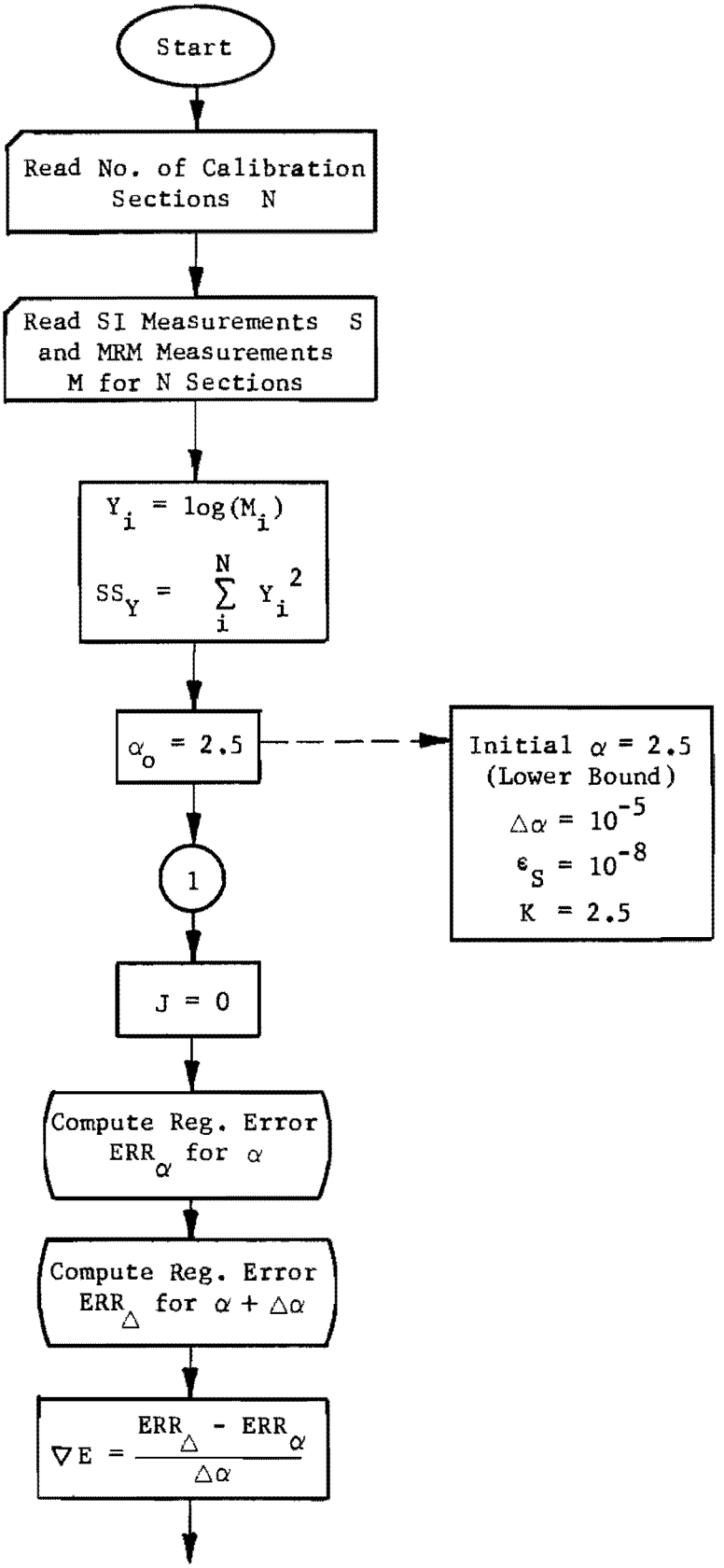

(Continued)

Fig A2.1. Flow chart for calibration procedure (Ref 10).

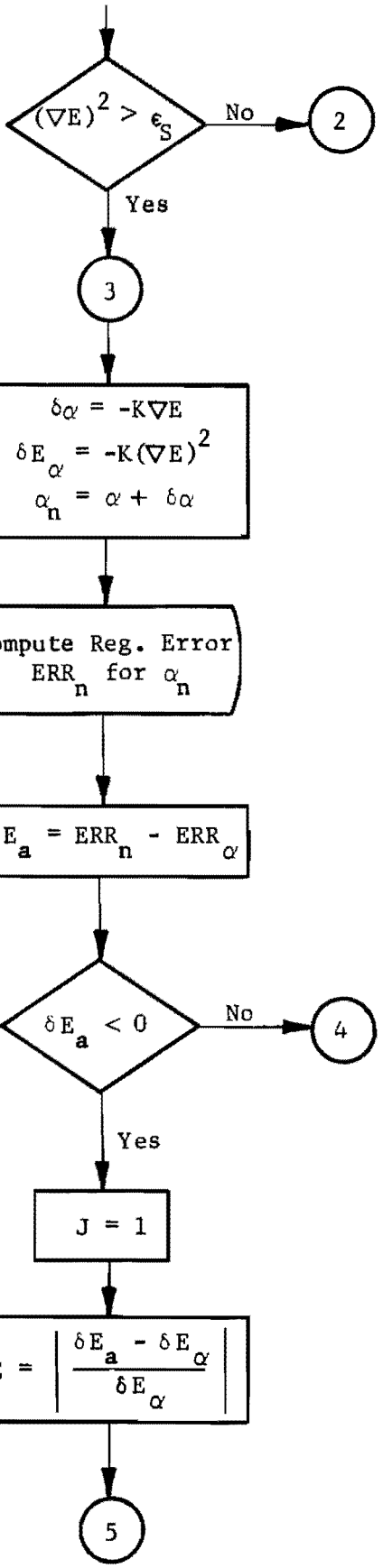

(Continued)

Fig A2.1. (Continued).

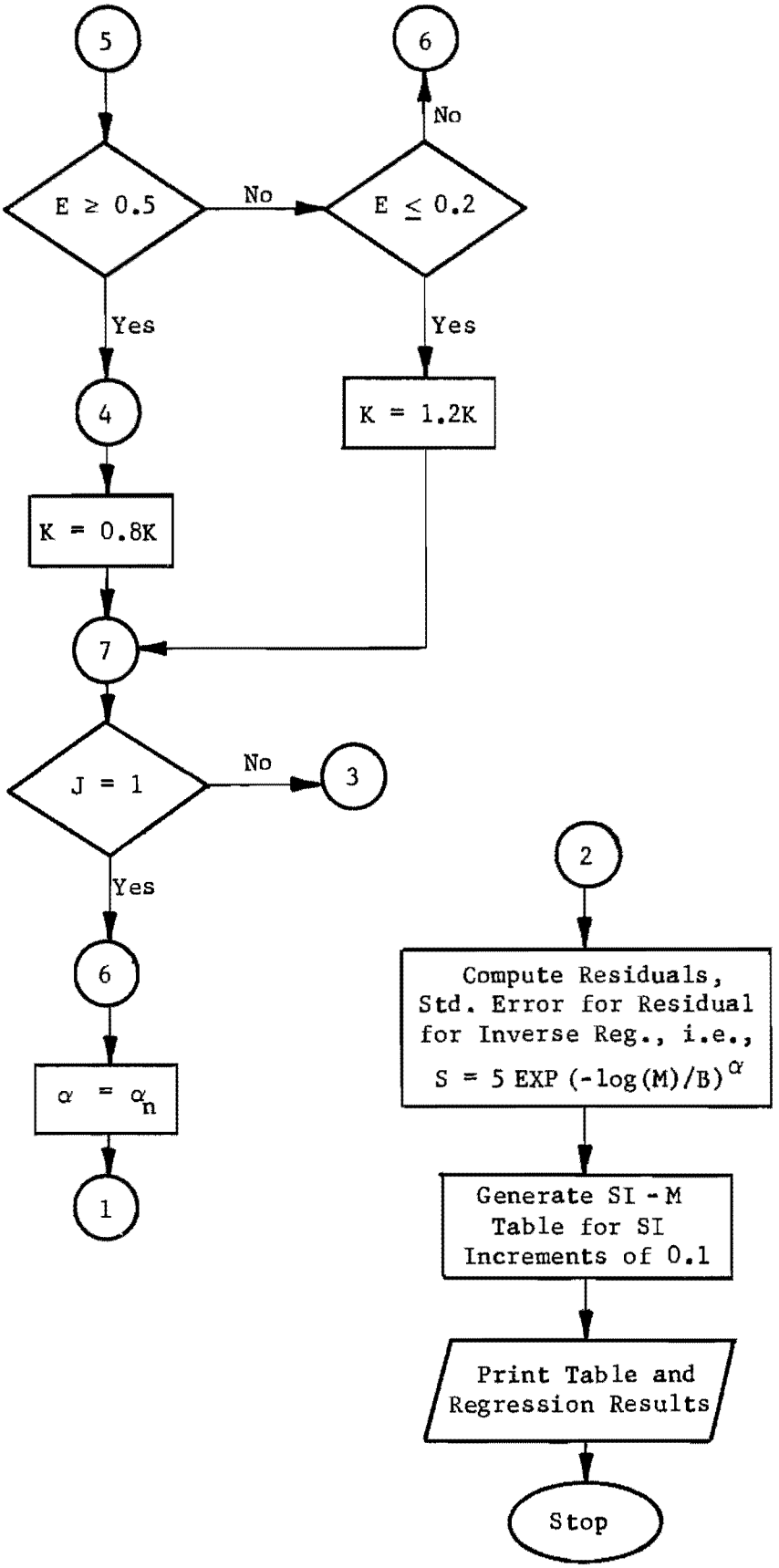

Fig A2.1. (Continued). (Continued)

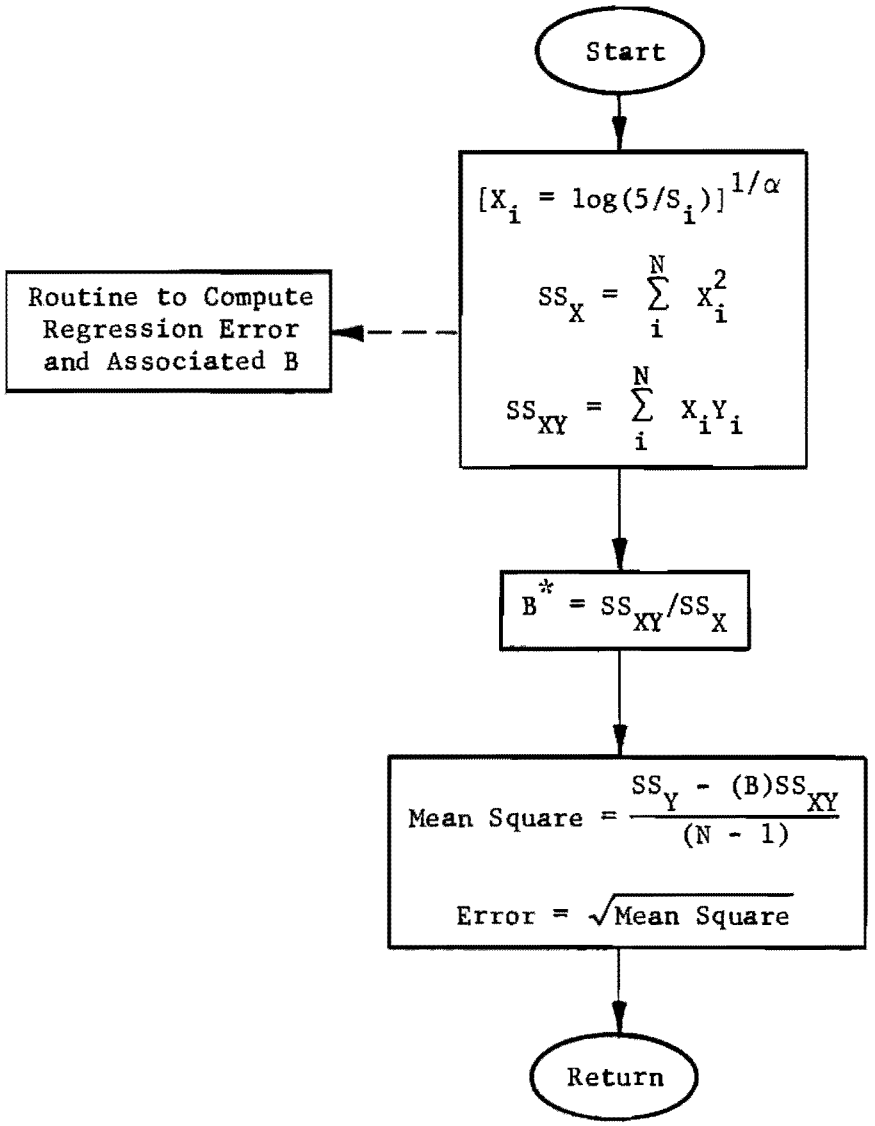

* Computational technique when model passes through origin.

Fig A2.1. (Continued).

THE AUTHORS

Roger S. Walker is an Assistant Professor of Computer Science at The University of Texas at Arlington. He was formerly a Research Engineer at the Center for Highway Research at The University of Texas at Austin. Before working at the Center for Highway Research, he had several years of experience in industry with Control Data Corporation and Radio Corporation of America. He is the author of several publications in transportation and computer systems.

W. Ronald Hudson is a Professor of Civil Engineering and Director of Research, Council for Advanced Transportation Studies at The University of Texas at Austin. He has had a wide variety of experience as a research engineer with the Texas Highway Department and the Center for Highway Research at The University of Texas at Austin and was Assistant Chief of the Rigid Pavement Research Branch of the AASHO Road Test. He is the author of numerous publications and was the recipient of the 1967 ASCE J. James R. Croes Medal. He is presently concerned with research in the areas of (1) analysis and design of pavement management systems, (2) measurement of pavement roughness performance, (3) slab analysis and design, and (4) tensile strength of stabilized subbase materials.